This is the peer-reviewed, final accepted version for American Mineralogist, published by the Mineralogical Society of America.
The published version is subject to change. Cite as Authors (Year) Title. American Mineralogist, in press.
DOI: https://doi.org/10.2138/am-2021-7593. http://www.minsocam.org/

Revision 3

Amphibole as a witness of chromitite formation and fluid metasomatism in ophiolites

Qi-Qi Pan [1, 2, 3*], Yan Xiao [1, 2*], Ben-Xun Su [2, 3, 4], Xia Liu [2, 3, 4], Paul T. Robinson [4], Ibrahim Uysal [5], Peng-Fei Zhang [6], Patrick Asamoah Sakyi [7]

[1] State Key Laboratory of Lithospheric Evolution, Institute of Geology and Geophysics, Chinese Academy of Sciences, Beijing 100029, China

[2] Innovation Academy for Earth Science, Chinese Academy of Sciences, Beijing 100029, China

[3] University of Chinese Academy of Sciences, Beijing 100049, China

[4] Key Laboratory of Mineral Resources, Institute of Geology and Geophysics, Chinese Academy of Sciences, Beijing 100029, China

[5] Department of Geological Engineering, Karadeniz Technical University, 61080-Trabzon, Turkey

[6] Department of Earth Sciences, the University of Hong Kong, Pokfulam Road, Hong Kong, China

[7] Department of Earth Science, School of Physical and Mathematical Sciences, University of Ghana, P. O. Box LG 58, Legon-Accra, Ghana

[*] Corresponding authors:
E-mail address: panqiqi@mail.iggcas.ac.cn (Q.Q. Pan);
xiaoyan@mail.iggcas.ac.cn (Y. Xiao)

Always consult and cite the final, published document. See http:/www.minsocam.org or GeoscienceWorld

This is the peer-reviewed, final accepted version for American Mineralogist, published by the Mineralogical Society of America.
The published version is subject to change. Cite as Authors (Year) Title. American Mineralogist, in press.
DOI: https://doi.org/10.2138/am-2021-7593. http://www.minsocam.org/

ABSTRACT

Here we present new occurrences of amphibole in a suite of chromitites, dunites and harzburgites from the mantle sequence of the Lycian ophiolite in the Tauride Belt, SW Turkey. The amphibole occurs both as interstitial grains among the major constituent minerals and as inclusions in chromite grains. The interstitial amphibole shows generally decreasing trends in Na_2O and Al_2O_3 contents from the chromitites (0.14 – 1.54 wt%; 0.04 – 6.67 wt%, respectively) and the dunites (0.09 – 2.37 wt%; 0.12 – 11.9 wt%) to the host harzburgites (< 0.61 wt%; 0.02 – 5.41 wt%). Amphibole inclusions in chromite of the amphibole-bearing harzburgites are poorer in Al_2O_3 (1.12 – 8.86 wt%), CaO (8.47 – 13.2 wt%) and Na_2O (b.d.l. – 1.38 wt%) than their counterparts in the amphibole-bearing chromitites (Al_2O_3 = 6.13 – 10.0 wt%; CaO = 12.1 – 12.9 wt%; Na_2O = 1.11 – 1.91 wt%). Estimated crystallization temperatures for the interstitial amphibole grains and amphibole inclusions range from 706 to 974 °C, with the higher values in the latter. A comparison of amphibole inclusions in chromite with interstitial grains provides direct evidence for the involvement of water in chromitite formation and the presence of hydrous melt/fluid metasomatism in the peridotites during initial subduction of Neo-Tethyan oceanic lithosphere. The hydrous melts/fluids were released from the chromitites after being collected on chromite surfaces during crystallization. Different fluid/wall rock ratios are thought to have controlled the crystallization and composition of the Lycian amphibole and the extent of modification of the chromite and pyroxene grains in the peridotites. Considering the wide distribution of podiform chromitites in this ophiolite, the link

Always consult and cite the final, published document. See http:/www.minsocam.org or GeoscienceWorld

This is the peer-reviewed, final accepted version for American Mineralogist, published by the Mineralogical Society of America.
The published version is subject to change. Cite as Authors (Year) Title. American Mineralogist, in press.
DOI: https://doi.org/10.2138/am-2021-7593. http://www.minsocam.org/

between chromitite formation and melt/fluid metasomatism defined in our study may be applicable to other ophiolites worldwide.

Keywords: Amphibole; Peridotite; Chromitite; Hydrous fluid; Ophiolite

INTRODUCTION

Podiform chromitites are a special category of chrome ore deposit found only in ophiolites, where they typically form just below the petrologic Moho (Cassard et al., 1981; Zhou et al., 1994). Hydrous fluids are widely thought to have played a vital role in chromitite formation in ophiolites (e.g., Matveev and Ballhaus, 2002; Johan et al., 2017; Su et al., 2020, 2021), and they are commonly preserved as fluid inclusions and/or hydrous minerals (such as phlogopite and amphibole) in the chromite grains of chromitites, dunites and harzburgites (Melcher et al., 1997; Sachan et al., 2007; Zhou et al., 2014; Rollinson et al., 2018). These hydrous minerals and fluid inclusions are considered to represent crystallization products of trapped melts which were clearly hydrous and estimated to have contained up to 4 wt% water (Sobolev and Chaussidon, 1996; Falloon and Danyushevsky, 2000; Matveev and Ballhaus, 2002). However, recent studies have proposed that post-magmatic processes (e.g., hydrothermal alteration, metamorphism) locally aided by deformation, could modify the original composition of chromite in chromitites (e.g., Rassios and Smith, 2000; Satsukawa et al., 2015; Kapsiotis et al., 2019). Such processes could also potentially produce hydrous inclusions in

Always consult and cite the final, published document. See http:/www.minsocam.org or GeoscienceWorld

DOI: https://doi.org/10.2138/am-2021-7593. http://www.minsocam.org/

chromite during sub-solidus annealing (e.g., Lorand and Ceuleneer, 1989). Therefore, the role of water in the formation of chromitite in ophiolite is still unclear.

Although interstitial amphibole crystals have rarely been reported in ophiolitic chromitite (Melcher et al., 1997; Rollinson, 2008), they have been increasingly found in ophiolitic peridotites (e.g., Liu et al., 2010; Rospabé et al., 2017; Çelik et al., 2018; Slovenec and Šegvić, 2018), fore-arc peridotites (e.g., Chen and Zeng, 2007; Nozaka, 2014) and mantle-wedge peridotite xenoliths (e.g., Coltorti et al., 2004; Ionov, 2010). The amphibole in these peridotites has mostly been attributed to hydrous fluid/melt metasomatism related to subduction processes. Thus, determining the potential links between fluid metasomatism in peridotites, the formation of podiform chromitites and water extracted from subducting slabs could provide additional insights into the role and source(s) of fluids involved in these processes.

In this contribution, we report a newly discovered suite of interstitial amphibole grains in chromitite, dunite and harzburgite in the mantle section of the Lycian ophiolite in SW Turkey. The occurrence and mineral chemistry of the amphibole reveal that the hydrous fluids were intimately related to chromitite formation and were subsequently infiltrated into the surrounding dunite and harzburgite.

GEOLOGY OF THE LYCIAN OPHIOLITE

The ophiolites in SW Anatolia, which lie along the westernmost part of the Tauride Belt, are widely interpreted to be part of a Tethyan suture zone (Fig. 1a). The western

Always consult and cite the final, published document. See http:/www.minsocam.org or GeoscienceWorld

This is the peer-reviewed, final accepted version for American Mineralogist, published by the Mineralogical Society of America.
The published version is subject to change. Cite as Authors (Year) Title. American Mineralogist, in press.
DOI: https://doi.org/10.2138/am-2021-7593. http://www.minsocam.org/

Taurides can be subdivided into three main geological units: the Beydağlari autochthon, comprising a thick platform of shallow-marine carbonates of Liassic to Early Miocene age with an unknown crustal basement; the Antalya nappe, emplaced westwards in the Late Cretaceous; and the younger Lycian nappe complex emplaced to the southeast. The Lycian ophiolite is mainly exposed in the Köyceğiz (Muğla) and Yeşilova (Burdur) regions (Fig. 1b, c) where it consists, from the base upward, of ophiolitic mélange, metamorphic sole, and mantle tectonites (Fig. 1d). The ophiolite mélange consists of radiolarian chert, siliceous marble, serpentinite, amphibolite, basalt, gabbro and peridotite within a highly deformed matrix of conglomerate, shale and lithic arenite (Collins and Robertson, 1998). The metamorphic sole exhibits an inverted metamorphic gradient from the top downward of pyroxene-bearing amphibolite, amphibolite, epidote-amphibolite and mica schist (Çelik, 2002; Çelik and Delaloye, 2003). $^{40}Ar/^{39}Ar$ dates of the amphibolites and mica schists indicate that tectonic displacement of the oceanic lithosphere occurred during the Late Cretaceous (ca. 91 – 94 Ma; Çelik et al., 2006). Above the metamorphic sole the ophiolite consists exclusively of mantle tectonites hosting podiform chromitites enclosed in dunite envelopes (Collins and Robertson, 1998; Çelik and Delaloye, 2003; Uysal et al., 2005, 2009, 2012). The mantle tectonites are intruded by isolated pockets of partially brecciated diabase, but otherwise crustal lithologies are typically absent in the ophiolite.

A suite of amphibole-bearing rocks was collected from the mantle section of the ophiolite in the Köyceğiz region bounded by coordinates 29°1′21″E – 29°10′29″E

Always consult and cite the final, published document. See http:/www.minsocam.org or GeoscienceWorld

This is the peer-reviewed, final accepted version for American Mineralogist, published by the Mineralogical Society of America.
The published version is subject to change. Cite as Authors (Year) Title. American Mineralogist, in press.
DOI: https://doi.org/10.2138/am-2021-7593. http://www.minsocam.org/

longitude and 36°42′11″N – 36°50′32″N latitude (Fig. 1b). The samples include nine chromitites, two dunites enveloping the chromitites and six harzburgite hosts. Most of the samples are overprinted by varying degrees of serpentinization. The degree of serpentinization decreases from chromitite and dunite to harzburgite, leaving considerable amounts of pristine olivine, pyroxene and amphibole in the harzburgite. Amphibole occurs as interstitial, mostly euhedral, grains between the major minerals or as anhedral crystals rimming clinopyroxene. Amphibole also occurs as inclusions in chromite grains from both the chromitites and harzburgites.

ANALYTICAL METHODS

All the samples with polished sections were investigated by a FEI Nova NanoSEM 450, equipped with an energy dispersive X-ray spectrometer from Oxford Instruments at the Institute of Geology and Geophysics, Chinese Academy of Sciences (IGGCAS), Beijing, China. High-resolution back-scattered electron (BSE) images were obtained at working conditions of 15 kV accelerating voltage and 5.5 nA beam current, with a working distance of 6 mm from the pole piece to the sample surface. The spatial resolution of the BSE scanning was approximately 2 μm per pixel. Areas ranging from half to whole thin sections were mapped. Mineral modes of chromitite and dunite were determined from BSE images using Adobe Photoshop and ImageJ software. The spatial distribution of different minerals in the images were resolved using Adobe Photoshop based on their difference in brightness and contrast. Then, an image showing the

Always consult and cite the final, published document. See http:/www.minsocam.org or GeoscienceWorld

This is the peer-reviewed, final accepted version for American Mineralogist, published by the Mineralogical Society of America.
The published version is subject to change. Cite as Authors (Year) Title. American Mineralogist, in press.
DOI: https://doi.org/10.2138/am-2021-7593. http://www.minsocam.org/

distribution of each mineral was imported into ImageJ to analyze the modal percentages. However, olivine and orthopyroxene are difficult to distinguish in harzburgite because of their similar brightness and contrast in BSE images. Thus, the mineral modes of harzburgite were determined by point counting (1000 counts for areas of 2.5 × 4.5 cm). The pixel/point-counting data are listed in Table 1.

Major element compositions of minerals and back scattered electron images of samples were obtained using a JEOL JXA8100 electron probe microanalyzer (EPMA) at the IGGCAS. The analyses were carried out at an accelerating voltage of 15 kV, a beam current of 10 nA and a 10 – 30 s counting time on peak. A beam diameter of 5 μm was used for interstitial minerals and 1 μm for mineral inclusions. Well-characterized natural minerals and synthetic oxides were used for standard calibration. Raw data were reduced with an EPMA online correction procedure, including background, dead time and a ZAF-correction program. Accuracy and precision were checked against SPI standards. Typical analytical accuracy for all the elements analyzed was better than 2%. Detection limits (in wt%) of oxides were as follows: SiO_2 0.01; TiO_2 0.02; Al_2O_3 0.01; Cr_2O_3 0.03; FeO 0.01; MnO 0.06; MgO 0.06; CaO 0.02; Na_2O 0.03; K_2O 0.02; and NiO 0.03. The $Fe^{3+}/\sum Fe$ ratio of chromite was calculated based on microprobe analyses using stoichiometric criteria (Droop, 1985). Amphibole formulas were calculated from the microprobe analyses using the method of Ridolfi et al. (2018) for apportioning the amount of Fe^{3+}. Classification of amphibole is based on the chemical contents of the standard amphibole formula $AB_2C_5^{VI}T_8^{IV}O_{22}(OH)_2$ (Leake et al., 1997). At least three

Always consult and cite the final, published document. See http:/www.minsocam.org or GeoscienceWorld

grains of each mineral were analyzed in each thin section, and at least two points were analyzed in the cores and rims of each crystal. The results of olivine, clinopyroxene, orthopyroxene and chromite are reported in Table 2 and amphibole in Table 3.

PETROGRAPHY AND MINERAL CHEMISTRY

Amphibole occurrences

The amphibole-bearing chromitites have mostly disseminated, massive and nodular textures, and consist of chromite (20 – 80 modal%); olivine (78 – 18 %); amphibole (< 2 %); ± clinopyroxene (< 1 %) (Table 1 and Fig. 2a-h). Amphibole in the chromitites occurs either as interstitial phases (mostly 0.2 – 0.3 mm; Fig. 2b, c, d, f, g) or as inclusions in chromite grains (Fig. 2h). The amphibole inclusions (2 – 40 μm across) are located well away from fractures, have globular to subhedral shapes and are either monomineralic or contain both amphibole and pyroxene (Fig. 2h).

The amphibole-bearing dunites have equigranular textures and contain 5 – 20 modal% euhedral to subhedral chromite grains. Silicate minerals include olivine (92 – 77 %); clinopyroxene (< 1 %); and amphibole (< 2 %) (Table 1 and Fig. 2i). Interstitial amphibole grains occur as minute crystals (0.1 – 0.5 mm) surrounding chromite grains (Fig. 2j) or intergrown with clinopyroxene (0.1 – 0.2 mm) (Fig. 2k). A few relatively large amphibole grains, up to 10 mm long (Fig. 2l), are present in some dunites near the chromitites (e.g., 18LN07-5).

Amphibole-bearing harzburgites have porphyroclastic textures, in which large

Always consult and cite the final, published document. See http:/www.minsocam.org or GeoscienceWorld

This is the peer-reviewed, final accepted version for American Mineralogist, published by the Mineralogical Society of America.
The published version is subject to change. Cite as Authors (Year) Title. American Mineralogist, in press.
DOI: https://doi.org/10.2138/am-2021-7593. http://www.minsocam.org/

orthopyroxene porphyroclasts (> 2 mm) are surrounded by small neoblasts (≤ 0.5 mm) (Table 1 and Fig. 3a-l). The harzburgite consists mainly of olivine (~ 85 modal%) and orthopyroxene (~ 10 %), accompanied by minor amounts of clinopyroxene (< 3 %); chromite (< 2 %); and amphibole (< 2 %). Two types of amphibole have been identified in these rocks: 1) Small (< 0.1 mm) interstitial grains rimming clinopyroxene and orthopyroxene crystals (Fig. 3b, c, g, k) or larger, anhedral crystals (mostly 0.3 – 0.4 mm) among the olivine grains (Fig. 3d, f, j); and 2) rounded inclusions in chromite grains that range from 5 – 50 μm and that are either monophase or multiphase with orthopyroxene and clinopyroxene (Fig. 3h, l). Some of the inclusions are cut by cracks that extend into the host chromite (Fig. 3l). Minerals in the inclusions far from cracks show little or no alteration.

Mineral chemistry

Olivine. Olivine grains in the amphibole-bearing chromitites have Fo (=100Mg/(Mg+Fe^{2+})) values ranging from 94.7 to 96.9 and NiO contents from 0.50 to 0.77 wt%. The two amphibole-bearing dunite samples contain olivine grains with lower Fo values of 92.8 – 95.0 and NiO contents of 0.36 – 0.53 wt% (Fig. 4a). In the amphibole-bearing harzburgites, the olivine grains show limited ranges of Fo (90.8 – 91.6) and NiO (0.24 – 0.43 wt%), comparable in composition to olivine in harzburgites from the Lycian ophiolite (Aladanmaz et al., 2009; Uysal et al., 2012; Xiong et al., 2018b) and plotting the fore-arc peridotite field and the olivine mantle array (Fig. 4a).

Always consult and cite the final, published document. See http:/www.minsocam.org or GeoscienceWorld

This is the peer-reviewed, final accepted version for American Mineralogist, published by the Mineralogical Society of America.
The published version is subject to change. Cite as Authors (Year) Title. American Mineralogist, in press.
DOI: https://doi.org/10.2138/am-2021-7593. http://www.minsocam.org/

Pyroxene. Orthopyroxene grains occur only in the amphibole-bearing harzburgite and have Mg# values of 90.7 – 92.1 (Table 2), overlapping the range of those reported in previous studies (Aldanmaz et al., 2009; Uysal et al., 2012; Xiong et al., 2018b). In contrast, their Al_2O_3 contents of 0.40 – 2.58 wt% are slightly lower than those in the orthopyroxene reported by Aldanmaz et al. (2009) (1.43 – 4.62 wt%) and Uysal et al. (2012) (1.09 – 5.21 wt%) (Fig. 4b), but are similar to those in Xiong et al. (2018b) (0.70 – 1.90 wt%).

The interstitial clinopyroxene grains in the amphibole-bearing chromitites have nearly uniform Mg# values (97.1 – 98.2) and CaO contents (24.1 – 25.3 wt%) but variable Al_2O_3 (0.16 – 0.52 wt%) and Na_2O (0.15 – 0.26 wt%) (Fig. 4b). In comparison, clinopyroxene grains in both amphibole-bearing dunites and harzburgites display significantly lower Mg# values of 95.8 – 97.0 and 93.5 – 95.7 and Na_2O contents of 0.09 – 0.20 wt% and < 0.09 wt%, respectively. Their Al_2O_3 contents vary from 0.21 to 0.67 wt% and 0.21 to 3.19 wt%, respectively, slightly lower than those in amphibole-free peridotites reported in previous studies (Fig. 4b).

Chromite. Similar to previously described chromite in the Lycian ophiolite (Uysal et al., 2005, 2009), chromite grains in the massive, amphibole-bearing podiform chromitites show highly variable TiO_2 contents of 0.08 – 0.23 wt% and Cr# values (=100Cr/(Cr+Al)) of 58.4 – 81.5. Thus, the chromitites are mostly high-Cr varieties (Cr# > 60) that formed from boninitic melts (Uysal et al., 2005; Xiong et al., 2018a). Chromite grains in the amphibole-bearing dunites have narrow Cr# variations (79.2 –81.5), within

Always consult and cite the final, published document. See http:/www.minsocam.org or GeoscienceWorld

This is the peer-reviewed, final accepted version for American Mineralogist, published by the Mineralogical Society of America.
The published version is subject to change. Cite as Authors (Year) Title. American Mineralogist, in press.
DOI: https://doi.org/10.2138/am-2021-7593. http://www.minsocam.org/

the range of those in amphibole-free dunites (Uysal et al., 2012; Xiong et al., 2018b). In contrast, chromite grains in the amphibole-bearing harzburgites have relatively variable Cr# values (37.8 – 73.1), which correlate negatively with their Mg# values and plot in the fore-arc peridotite field (Fig. 4c).

Amphibole. In amphibole-bearing chromitites, interstitial amphibole grains are mostly tremolite and magnesiohornblende (Fig. 5). They have variable contents of Na_2O (0.14 – 1.54 wt%), CaO (9.86 – 13.4 wt%), Al_2O_3 (0.04 – 6.67 wt%) and Mg# values of 96.5 – 99.7 (Fig. 6a; Table 3), overlapping the ranges of amphibole in the Oman ophiolite (Rollinson, 2008). Interstitial amphibole grains in the dunites are tremolite and magnesiohornblende, with a few edenite varieties (Fig. 5). They display larger variations in Na_2O (0.09 – 2.37 wt%), Al_2O_3 (0.12 – 11.9 wt%) and Mg# values (93.1 – 99.1) than those in the chromitites. The interstitial amphibole grains in harzburgites are tremolite with generally lower Na_2O (< 0.61 wt%), Al_2O_3 (0.02 – 5.41 wt%) and Mg# values (93.7 – 96.4) (Figs. 5a, b, 6a; Table 3).

Amphibole inclusions in chromite mainly range from magnesiohornblende to tremolite, but two analyses yielded edenite compositions (Fig. 5). Compared to the interstitial amphibole, the amphibole inclusions exhibit higher Al_2O_3 and Na_2O contents and lower Mg# values (Fig. 6a, b; Table 3). The amphiboles in the harzburgites are poorer in Al_2O_3 (1.12 – 8.86 wt%), CaO (8.47 – 13.2 wt%) and Na_2O (b.d.l. – 1.38 wt%) contents than their counterparts in the chromitites (Al_2O_3 = 6.13 – 10.0 wt%; CaO = 12.1 – 12.9 wt%; Na_2O = 1.11 – 1.91 wt%).

Always consult and cite the final, published document. See http:/www.minsocam.org or GeoscienceWorld

DISCUSSION

The petrographic and mineral chemical data presented here demonstrate that considerable amounts of amphibole occur as interstitial grains and as inclusions in chromite in some of the chromitites, dunites and harzburgites of the mantle section of the Lycian ophiolite. In the following, we first discuss the effects of deformation during post-magmatic processes on these rocks, and then explore the origin of the amphibole in them. We then consider possible sources of the fluids from which the amphibole formed and investigate the importance of fluids in the formation of inclusions in chromite. Finally, we address the role that the fluids played in the evolution of the Lycian ophiolite.

The effect of deformation during the post-magmatic evolution on the Lycian ophiolite mantle sequence

Podiform chromitites in ophiolites are normally surrounded by dunite envelopes of variable thickness within mantle harzburgite (Cassard et al., 1981; Lago et al., 1982). For the fluids to penetrate the massive rocks and lead to crystallization of interstitial amphibole, they must have been warm and the rocks must have had significant permeability (Angiboust et al., 2012). Such conditions are expected to prevail only during early stages of crystallization when significant shearing or intrusive pathways would provide access for fluids into the rocks. According to field observations, the

Always consult and cite the final, published document. See http:/www.minsocam.org or GeoscienceWorld

harzburgite, dunite and chromitite in the Lycian ophiolite have undergone extensive, late-stage, solid-state fracture but little high temperature shearing (Fig. 7a).

Several studies reported that post-magmatic processes (e.g., hydrothermal alteration, metamoprhism) locally aided by deformation could alter chromitites and their surrounding peridotites. Because chromitite is more competent than dunite and harzburgite, dunite can preferentially accommodate more strain than the other lithologies as temperatures decrease (e.g., Rassios and Smith, 2000). As temperatures continue to decrease under sustained shear, dunite forms brittle shear zones which may serve as localized permeability pathways, enabling the migration of post-magmatic fluids (Kapsiotis et al., 2019). Such deformed chromitites typically have porphyroclastic textures consisting of coarse-grained porphyroclasts and fine-grained neoblasts (Passchier and Trouw, 2005; Satsukawa et al., 2015). In addition, chromite crystals affected by deformation are typically recognized by a presence of porous cores and rims (Colás et al., 2014) or multiphase ferritchromit rims (Mellini et al., 2005; Qiu and Zhu, 2017). However, the chromite grains in the chromitites of Lycian ophiolite have no porphyroclatic texture and are homogeneous without pores or core-rim textures (Fig. 2, 3, 7b, c). On the other hand, amphibole produced by post-magmatic processes is generally tremolite (Cannat and Seyler, 1995; Nozaka, 2005), commonly associated with serpentine and talc. Although tremolite is found in the Lycian amphibole-bearing chromitites, dunites and harzburgites, the common amphibole is euhedral and magnesiohornblende grading into edenite (Fig. 2, 3, 6a, c). Furthermore, the degree of

Always consult and cite the final, published document. See http:/www.minsocam.org or GeoscienceWorld

serpentinization in this study decreases from chromitite and dunite to the host harzburgite (Figs. 2, 3), indicating a high temperature, magmatic source for the fluids that penetrated outward. Meanwhile, the crystallization temperatures for both interstitial amphibole and amphibole inclusion, estimated using the geothermometer of Putirka (2016), range from 706 to 974 °C (Table 3), which are higher than those of deformed chromitites (500 – 700 °C; Satsukawa et al., 2015). Therefore, all these features indicate that the deformation during the post-magmatic evolution does not account for the formation of amphibole in the Lycian ophiolitic rocks.

Hydrous melt/fluid activity in the formation of ophiolitic chromitites and dunites

Parental melts of most chromitites in ophiolites are thought to be hydrous in nature as evidenced by the common presence of hydrous inclusions (e.g., amphibole, phlogopite and fluids) in chromite (e.g., Johan et al., 1983; McElduff and Stumpfl, 1991; Melcher et al., 1997; Schiano et al., 1997; Rollinson, 2008; Borisova et al., 2012; Zhou et al., 2014; Liu et al., 2018; Su et al., 2021). These hydrous minerals are characterized by enrichment in alkali components and CaO contents (Fig. 6b), which are widely considered to be favorable for Cr concentration and chromite precipitation (e.g., Pagé and Barnes, 2009; Uysal et al., 2016; Liu, X et al., 2018, 2019; Su et al., 2021). Our current investigation found that the chromitites and dunites in the Lycian ophiolite also have magmatic amphibole in their matrix, which is an uncommon occurrence previously reported only from the Kempirsai (Melcher et al., 1997) and Oman (Rollinson, 2008) ophiolites.

Always consult and cite the final, published document. See http:/www.minsocam.org or GeoscienceWorld

This is the peer-reviewed, final accepted version for American Mineralogist, published by the Mineralogical Society of America.
The published version is subject to change. Cite as Authors (Year) Title. American Mineralogist, in press.
DOI: https://doi.org/10.2138/am-2021-7593. http://www.minsocam.org/

Our findings in the Lycian chromitites provide direct evidence for the involvement of water in chromitite formation. However, at upper mantle or mantle-crust transition depths, where podiform chromitites commonly occur in most ophiolites hydrous minerals are rare. Instead, olivine and subordinate clinopyroxene are the common silicate phases in the chromitites (e.g., Lenaz et al., 2014; Rollinson and Adetunji, 2015; Chen et al., 2019; Su et al., 2019, 2020). The positively coupled variation between water contents in silicates and chromites implies that water in silicate minerals was probably derived from fluids extracted from the chromite surface (Su et al., 2020), thus, confirming the collection of fluid by chromite during crystallization as proposed by Matveev and Ballhaus (2002).

Chromitite and dunite formation in ophiolitic harzburgites is linked to fluid metasomatism

In contrast with amphibole in the Lycian chromitites and dunites, that in the harzburgites occurs as anhedral grains among the silicate minerals and has a close spatial relationship with clinopyroxene and chromite (Figs. 2, 3). These amphiboles have Mg# values similar to those of the clinopyroxene grains, but obviously higher than those of orthopyroxene and olivine (Fig. 9), implying a genetic affinity between the amphibole and clinopyroxene. These features suggest that the amphibole in the harzburgites was formed by reaction with hydrous melts/fluids, during which clinopyroxene was replaced (Ionov et al., 1997).

Always consult and cite the final, published document. See http:/www.minsocam.org or GeoscienceWorld

This is the peer-reviewed, final accepted version for American Mineralogist, published by the Mineralogical Society of America.
The published version is subject to change. Cite as Authors (Year) Title. American Mineralogist, in press.
DOI: https://doi.org/10.2138/am-2021-7593. http://www.minsocam.org/

Hydrous melts/fluids can have different origins, such as dehydration of a subducted plate (e.g., Ionov and Hofmann, 1995; Penniston-Dorland et al., 2012), hydrothermal fluids (Rospabé et al., 2017) and hydrous fluids that were collected on chromite grain surfaces (Matveev and Ballhaus, 2002; Su et al., 2020, 2021). The nature of metasomatizing agents can be identified by the chemical composition of the amphibole in the mantle peridotites (Ionov and Hofmann, 1995; Coltorti et al., 2004, 2007). Coltorti et al. (2007) revealed that amphibole in mantle xenoliths from subduction zones generally contains lower Na_2O and TiO_2 than those occurring in xenoliths from intraplate settings (Fig. 6a, b). In this study, most interstitial amphibole grains in the chromitite, dunite and harzburgite have lower Na_2O and higher SiO_2 contents than supra-subduction amphibole (S-Amp) and intraplate amphibole (I-Amp) (Fig. 6a), thus ruling out the possibility that the rocks were directly metasomatized by mantle-derived and subduction-related hydrous melts/fluids.

Rospabé et al. (2017) reported the presence of interstitial amphibole between olivine grains and amphibole inclusions in chromite grains from the dunitic transition zone (DTZ) of the Oman ophiolite. They interpreted the interstitial amphibole to have formed by hybridization between mid-oceanic ridge basaltic melt and high-temperature hydrothermal fluid. Those amphibole grains are rich in Na_2O (mostly 1.80 – 3.80 wt%), TiO_2 (mostly 0.03 – 0.80 wt%) and Al_2O_3 (mostly 8.33 – 15.6 wt%) but have relatively low Mg# values (82.6 – 93.1) (Rospabé et al., 2017). The amphiboles analyzed in this study have much lower Na_2O, TiO_2 and Al_2O_3 contents and higher Mg# values than those

Always consult and cite the final, published document. See http:/www.minsocam.org or GeoscienceWorld

in the DTZ of the Oman ophiolite (Fig. 6a, c, e). Thus, a hydrothermal origin for the Lycian amphibole can also be ruled out.

In the Lycian ophiolite, most olivine in the chromitites and dunites is partially or completely replaced by serpentine, especially that around chromite grains (Fig. 2b, c, d, f, g, j, k, l). Despite this, a considerable amount of pristine olivine is still present in the harzburgite (Fig. 3b, c, d, f, g, j, k). In the Lycian ophiolite, as in ophiolites worldwide, most chromitites are surrounded by dunite envelopes within the mantle harzburgites (Çelik and Delaloye, 2003; Uysal et al., 2005, 2012). In our study, the abundance of amphibole decreases from chromitite pod and dunite envelope to the host harzburgite in a trend similar to that observed for chromite. The amphibole grains in the chromitites and dunites are much more euhedral than those in the harzburgites (Fig. 2, 3). Thus, we interpret the podiform chromitites as basically crystal cumulates filling magma conduits and small chambers within the mantle peridotite (e.g., Lago et al., 1982). Generally, the Al_2O_3, TiO_2 and Na_2O contents of the amphibole grains also decrease from the chromitites and dunites to the harzburgites (Fig. 6a, c; Table 3) indicating that the fluids from which the amphibole grains crystallized penetrated outward from the chromitites and dunite envelopes to the harzburgites (Fig. 10). Su et al. (2020, 2021) suggested that the surface fluids on chromite grains would result in crystallization of clinopyroxene with high CaO (21.0 – 26.0 wt%) and SiO_2 (51.0 – 56.0 wt%) but low TiO_2 (< 0.40 wt%) compositions, which are similar to those in the Lycian chromitites (Fig. 4b; Table 2). Furthermore, the Mg# values of the amphibole grains are in equilibrium with

Always consult and cite the final, published document. See http:/www.minsocam.org or GeoscienceWorld

clinopyroxene in all three rock types (Fig. 9). Additionally, the interstitial amphibole grains are also calcic and have high SiO_2 and low TiO_2 contents. Thus, we propose that the amphibole grains in the Lycian chromitites and dunite were produced by direct crystallization from fluids originally trapped by the chromitites at high fluid/wall rock ratios. The heterogeneity of amphibole compositions and the presence of large amphibole grains (up to 10 mm) in the dunite might imply channelized flow of fluids. After crystallization of amphibole in the chromitite and dunite, the remaining fluids penetrated outward into the harzburgites (Fig. 10) and reacted with chromite and/or pyroxene to form amphibole at low fluid/rock ratios. The changing fluid/rock ratios may have controlled the mode of melt migration from ‘‘channelized flow’’ to ‘‘porous flow’’ as well as the amphibole compositions. The chromite grains in the Lycian harzburgites, particularly those enclosing amphibole and other phases, were most likely formed and/or modified by this mechanism (Fig. 10). In this respect, chromite in the ophiolitic harzburgites cannot be used as an indicator of partial melting due to the effect of metasomatism.

IMPLICATIONS

In addition to the interstitial amphiboles, many calcic amphiboles occur as inclusions in the chromite grains from both the chromitites and harzburgites. These inclusions are round to irregular in morphology and can be either single phase or multi-phase varieties intergrown with pyroxene (Figs. 2h, 3h, l). Many of these

Always consult and cite the final, published document. See http:/www.minsocam.org or GeoscienceWorld

inclusions contain several silicate phases and are therefore distinct from accidental inclusions of pre-existing, early-formed silicates such as olivine (Prichard et al., 2018). In addition, euhedral negative crystal inclusions are typical in chromite grains from Lycian chromitites and harzburgites. Several theories explain how negative crystal-shaped inclusions form, including entrapment of primary melt inclusions and annealing/sintering of multiple grains around pockets of trapped interstitial melt (Hulbert and Von Grunewald, 1985). The inclusions trapped during annealing/sintering are solitary inclusions, without crystallographic orientation with respect to chromite symmetry (Spry, 1969). Moreover, ductile deformation tend to generate neoblasts in response to recovery and dynamic recrystallization processes (e.g., Ghosh et al., 2014), which define a polygonal grain-boundary network with well-developed 120° triple (and sometimes 90° quadruple) junctions, giving locally rise to a typical annealing micro-structure (Kapsiotis et al., 2019). In some case, chromite neoblasts show irregular zoning patterns and are partly altered to ferrous chromite along their boundaries (Vukmanovic et al., 2013; Kapsiotis et al., 2019). However, the chromite grains in the Lycian chromitites and harzburgites are homogeneous and have no core-rim textures. Therefore, inclusions whose form and orientation were imposed by the structure of the host mineral are likely to be melt inclusions trapped during crystallization of the chromite.

Amphibole inclusions in chromite from the Lycian ophiolite have slightly lower Na_2O contents than those in inclusions from the DTZ and in ophiolitic chromitites (Fig. 6b and Table 3; Uysal et al., 2009; Borisova et al., 2012; Xiong et al., 2018b), but are

Always consult and cite the final, published document. See http:/www.minsocam.org or GeoscienceWorld

This is the peer-reviewed, final accepted version for American Mineralogist, published by the Mineralogical Society of America.
The published version is subject to change. Cite as Authors (Year) Title. American Mineralogist, in press.
DOI: https://doi.org/10.2138/am-2021-7593. http://www.minsocam.org/

similar to interstitial grains in the Lycian chromitites and harzburgites (Fig. 6a, b). The similar crystallization temperatures of the interstitial amphibole and that in the inclusions (Fig. 8) indicate that the two varieties most likely crystallized simultaneously. Thus, the amphibole inclusions in chromite likely had a similar origin as the coexisting interstitial amphibole. Due to the presence of surface hydrous fluids on chromite grains, the inclusions were probably derived from reaction between surface fluids and the captured melt.

It is not necessary for the captured melt to have specific amounts of water, because the water is concentrated on the surfaces of chromite grains during chromitite formation (Matveev and Ballhaus, 2002). These fluids were most likely released from the chromitites and infiltrated into the surrounding dunites and peridotites. Matveev and Ballhaus (2002) suggested that basaltic melts that produce chromite deposits should have H_2O contents high enough (up to 4 wt%) to exsolve a water-rich fluid phase. This is most likely to occur in supra-subduction zone environments. The rarity of interstitial amphibole in podiform chromitites and mantle peridotites of ophiolites worldwide is probably because amphibole in these rocks was unstable and preferentially melted or altered during multiple stages of melt metasomatism.

The well-preserved nature of the interstitial amphibole in the Lycian ophiolite implies rapid emplacement after crystallization. The Lycian ophiolite and other ophiolites in the Tauride Belt, as well as the Oman ophiolite, are characterized by short age gaps (generally less than 3 m.y.) between the ophiolite and its metamorphic sole, which is

Always consult and cite the final, published document. See http:/www.minsocam.org or GeoscienceWorld

This is the peer-reviewed, final accepted version for American Mineralogist, published by the Mineralogical Society of America.
The published version is subject to change. Cite as Authors (Year) Title. American Mineralogist, in press.
DOI: https://doi.org/10.2138/am-2021-7593. http://www.minsocam.org/

thought to record the time of initial subduction of the Neo-Tethyan oceanic lithosphere (e.g., Pearce et al., 1984; Robertson, 2002; Soret et al., 2017; Chen et al., 2018; Liu, X et al., 2019). Compared to other ophiolites, another typical feature of the Tauride ophiolites is the occurrence of pristine minerals in the peridotites, and particularly in the chromitites (e.g., Chen et al., 2019; Su et al., 2020, 2021). The interstitial amphibole and clinopyroxene grains in the chromitites are thought to have played a vital role in their formation. These grains could have absorbed most of the water in the melts/fluids, thereby mitigating hydration and serpentinization of olivine in the chromitites and the surrounding peridotites (Su et al., 2020). Because podiform chromitites are widely distributed in ophiolites worldwide, the linkage between chromitite formation and melt/fluid metasomatism, as observed in the Lycian ophiolite, may be applicable to other such bodies. As stated above, amphibole and clinopyroxene are rarely found in ophiolitic chromitites, but are relatively common in peridotites. Their compositions can be used to distinguish between different origins (Fig. 6) and thus, can be used to trace the metasomatic melt/fluid sources and to identify the mechanism of chromite mineralization.

ACKNOWLEDGMENTS

Constructive and detailed comments from two anonymous reviewers and the editor Sarah Penniston-Dorland are greatly appreciated. This study was financially supported

Always consult and cite the final, published document. See http:/www.minsocam.org or GeoscienceWorld

by the Second Tibetan Plateau Scientific Expedition and Research Program (STEP) (2019QZKK0801), the National Natural Science Foundation of China (Grants 91755205 and 41772055) and Youth Innovation Promotion Association, Chinese Academy of Sciences (2017095).

Always consult and cite the final, published document. See http:/www.minsocam.org or GeoscienceWorld

This is the peer-reviewed, final accepted version for American Mineralogist, published by the Mineralogical Society of America.
The published version is subject to change. Cite as Authors (Year) Title. American Mineralogist, in press.
DOI: https://doi.org/10.2138/am-2021-7593. http://www.minsocam.org/

REFERENCES CITED

Aldanmaz, E., Schmidt, M.W., Gourgaud, A., and Meisel, T. (2009) Mid-ocean ridge and supra-subduction geochemical signatures in spinel-peridotites from the Neotethyan ophiolites in SW Turkey: implications for upper mantle melting processes. Lithos, 113, 691-708.

Angiboust, S., Wolf, S., Burov, E., Agard, P., and Yamato, P. (2012) Effect of fluid circulation on subduction interface tectonic processes: Insights from thermo-mechanical numerical modelling. Earth and Planetary Science Letters, 357-358, 238-248.

Ballhaus, C., Berry, R.F., and Green, D.H. (1991) High pressure experimental calibration of the olivine-orthopyroxene-spinel oxygen geobarometer: implications for the oxidation state of the upper mantle. Contributions to Mineralogy and Petrology, 107, 27-40.

Borisova, A.Y., Ceuleneer, G., Kamenetsky, V.S., Arai, S., Béjina, F., Abily, B., Bindeman, I.N., Polvé, M., Parseval, P.D., Aigouy, T., and Pokrovski, G.S. (2012) A new view on the petrogenesis of the Oman ophiolite chromitites from microanalyses of chromite-hosted inclusions. Journal of Petrology, 53, 2411-2440.

Cannat, M., and Seyler, M. (1995) Transform tectonics, metamorphic plagioclase and amphibolitization in ultramafic rocks of the Vema transform fault (Atlantic Ocean). Earth and Planetary Science Letters, 133, 283-298.

Cassard, D., Nicolas, A., Rabinovitch, M., Moutte, J., Leblanc, M., and Prinzhofer, A. (1981) Structural classification of chromite pods in southern New Caledonia. Economic Geology 76, 805-831.

Çelik, Ö.F. (2002) Geochemical, petrological and geochronological observations on the metamorphic rocks of the Tauride Belt Ophiolites (S. Turkey). Published Ph.D. thesis, University of Geneva. Terre Environment, 39, 257.

Çelik, Ö.F., and Delaloye, M.F. (2003) Origin of metamorphic soles and their post-kinematic mafic dyke swarms in the Antalya and Lycian ophiolites, SW Turkey. Geological Journal, 38, 235-256.

Çelik, Ö.F., Delaloye, M.F., and Feraud, G. (2006) Precise ^{40}Ar-^{39}Ar ages from the metamorphic sole rocks of the Tauride Belt Ophiolites, southern Turkey: implications for the rapid cooling history. Geological Magazine, 143, 213-227.

Çelik, Ö.F., Marzoli, A., Marschik, R., Chiaradia, M., and Mathur, R. (2018) Geochemical, mineralogical and Re-Os isotopic constraints on the origin of Tethyan oceanic mantle and crustal rocks from the Central Pontides, northern Turkey. Mineralogy and Petrology, 112, 25-44.

Chen, C., Su, B.X., Jing, J.J., Xiao, Y., Lin, W., Chu, Y., Liu, X., and Bai, Y. (2018) Geological records of subduction initiation of Neo-Tethyan Ocean: ophiolites and metamorphic soles in southern Turkey. Acta Petrologica Sinica, 34, 3302-3314 (in Chinese with English abstract).

Always consult and cite the final, published document. See http:/www.minsocam.org or GeoscienceWorld

This is the peer-reviewed, final accepted version for American Mineralogist, published by the Mineralogical Society of America.
The published version is subject to change. Cite as Authors (Year) Title. American Mineralogist, in press.
DOI: https://doi.org/10.2138/am-2021-7593. http://www.minsocam.org/

Chen, C., Su, B.X., Xiao, Y., Pang, K.N., Robinson, P.T., Uysal, I., Lin, W., Qin, K.Z., Avcı, E., and Kapsiotis, A. (2019) Intermediate chromitite in Kızıldağ ophiolite (SE Turkey) formed during subduction initiation in Neo-Tethys. Ore Geology Reviews, 104, 88-100.

Chen, J., and Zeng, Z. (2007) Metasomatism of the peridotites from southern Mariana fore-arc: Trace element characteristics of clinopyroxene and amphibole. Science in China Series D: Earth Sciences, 50, 1005-1012.

Colás, V., González-Jimenéz, J.M., Grifn, W.L., Fanlo, I., Gervilla, F., O'Reilly, S.Y., Pearson, N.J., Kerestedjian, T., and Proenza, J.A. (2014) Fingerprints of metamorphism in chromite: new insights from minor and trace elements. Chemical Geology, 389, 137-152.

Collins, A.S., and Robertson, A.H.F. (1998) Processes of Late Cretaceous to Late Miocene episodic thrust-sheet translation in the Lycian Taurides, SW Turkey. Journal of the Geological Society, 155, 759-772.

Coltorti, M., Beccaluva, L., and Bonadiman, C. (2004) Amphibole genesis via metasomatic reaction with clinopyroxene in mantle xenoliths from Victoria Land, Antarctica. Lithos, 75, 115-139.

Coltorti, M., Bonadiman, C., and Faccini, B. (2007) Amphiboles from suprasubduction and intraplate lithospheric mantle. Lithos, 99, 68-84.

Droop, G.T.R. (1985) A general equation for estimating Fe^{3+} concentrations in ferromagnesian silicates and oxides from microprobe analyses, using stoichiometric criteria. Mineralogical magazine, 361, 431-435.

Falloon, T.J., and Danyushevsky, L.V. (2000) Melting of refractory mantle at 1.5, 2 and 2.5 GPa under anhydrous and H_2O undersaturated conditions; implications for the petrogenesis of high-Ca boninites and the influence of subduction components on mantle melting. Journal of Petrology, 41, 257-283.

GDMRE (General Directorate of Mineral Research and Exploration), (2002) 1:500.000 scaled Geological Maps of Turkey (Denizli map section), Ankara-Turkey.

Ghosh, B., Ray, J., and Morishita, T. (2014) Grain-scale plastic deformation of chromite from podiform chromitite of the Naga-manipur ophiolite belt, India: implication for mantle dynamics. Ore Geology Reviews, 56, 199-208.

Huang, Y., Wang, L., Kusky, T., Robinson, P.T., Peng, S., Polat, A., and Deng, H. (2017) High-Cr chromites from the late Proterozoic Miaowan Ophiolite Complex, South China: implications for its tectonic environment of formation. Lithos, 288, 35-54.

Hulbert, L.J., and Von Gruenewaldt, G. (1985) Textural and compositional features of chromite in the lower and critical zones of the Bushveld complex South of Potgietersrus. Economic Geology, 80, 872-895.

Ionov, D.A., and Hofmann, A.W. (1995) Nb-Ta-rich mantle amphiboles and micas: implications for subduction-related metasomatic trace element fractionations. Earth and Planetary Science Letters, 131, 341-356.

Ionov, D.A., Griffin, W.L., and O'Reilly, S.Y. (1997) Volatile-bearing minerals and

Always consult and cite the final, published document. See http:/www.minsocam.org or GeoscienceWorld

lithophile trace elements in the upper mantle. Chemical Geology, 141, 153-184.

Ionov, D.A. (2010) Petrology of mantle wedge lithosphere: new data on supra-subduction zone peridotite xenoliths from the andesitic Avacha volcano, Kamchatka. Journal of Petrology, 51, 327-361.

Ishii, T., (1992) Petrological studies of peridotites from diapiric serpentinite seamounts in the Izu Ogasawara-Mariana forearc, Leg 125. Proceedings of the Ocean Drilling Program, Scientific Results. Ocean Drilling Program, 125, 401-414.

Johan, Z., Dunlop, H., Le Bel, L., Robert, J.L., and Volfnger, M. (1983) Origin of chromite deposits in ophiolitic complexes: evidence for a volatile- and sodium-rich reducing fluid phase. Fortschritte der Mineralogie, 61, 105-107.

Johan, Z., Martin, R.F., and Ettler, V. (2017) Fluids are bound to be involved in the formation of ophiolitic chromite deposits. European Journal of Mineralogy, 29, 543-555.

Kapsiotis, A., Economou-Eliopoulos, M., Zheng, H., Su, B.X., Lenaz, D., Jing, J.J., Antonelou, A., Velicogna, M., and Xia, B. (2019) Refractory chromitites recovered from the Eretria mine, East Othris massif (Greece): Implications for metallogeny and deformation of chromitites within the lithospheric mantle portion of a forearc-type ophiolite. Geochemistry, 79, 130-152.

Khedr, M.Z., Arai, S., Python, M., and Tamura, A. (2014) Chemical variations of abyssal peridotites in the central Oman ophiolite: evidence of oceanic mantle heterogeneity. Gondwana Research, 25, 1242-1262.

Lago, B.L., Rabinowicz, M., Nicolas, A. (1982) Podiform chromitite ore bodies: a genetic model. Journal of Petrology, 23, 103-125.

Leake, B.E., Woolley, A.R., and Arps, C.E.S. (1997) Nomenclature of amphiboles. Reports of the subcommittee on amphiboles of the International Mineralogical Association Commission on new minerals and mineral names. European Journal of Mineralogy, 9, 623-651.

Lenaz, D., Adetunji, J., and Rollinson, H. (2014) Determination of $Fe^{3+}/\sum Fe$ ratios in chrome spinels using a combined Mössbauer and single-crystal X-ray approach: application to chromitites from the mantle section of the Oman ophiolite. Contributions to Mineralogy and Petrology, 167, 1-17.

Liu, C.Z., Wu, F.Y., Wilde, S.A., Yu, L.J., and Li, J.L. (2010) Anorthitic plagioclase and pargasitic amphibole in mantle peridotites from the Yungbwa ophiolite (southwestern Tibetan Plateau) formed by hydrous melt metasomatism. Lithos, 114, 413-422.

Liu, J.G., Hattori, K., and Wang, J. (2017) Mineral inclusions in chromite from the chromite deposit in the Kudi ophiolite, Tibet, Proto-Tethys. Acta Geologica Sinica-English Edition, 91, 469-485.

Liu, T., Wu, F.Y., Liu, C.Z., Zhang, C., Ji, W.B., and Xu, Y. (2019) Reconsideration of Neo-Tethys evolution constrained from the nature of the Dazhuqu ophiolitic mantle, southern Tibet. Contributions to Mineralogy and Petrology, 174, 23.

Always consult and cite the final, published document. See http:/www.minsocam.org or GeoscienceWorld

Liu, X., Su, B.X., Bai, Y., Chen, C., Xiao, Y., Liang, Z., Yang, S.H., Peng, Q.S., Su, B.C., and Liu, B. (2018) Ca-enrichment characteristics of parental magmas of chromitite in ophiolite: inference from mineral inclusions. Earth Science, 43, 1038-1050 (in Chinese with English abstract).

Liu, X., Su, B.X., Xiao, Y., Chen, C., Uysal, I., Jing, J.J., Zhang, P.F., Chu, Y., Lin, W., and Sakyi, P.A. (2019) Initial subduction of Neo-Tethyan Ocean: Geochemical records in chromite and mineral inclusions in the Pozantı-Karsantı ophiolite, southern Turkey. Ore Geology Reviews, 110, 102926.

Lorand, J.P., and Ceuleneer, G. (1989) Silicate and base-metal sulfide inclusions in chromites from the Maqsad area (Oman ophiolite, Gulf of Oman): a model for entrapment. Lithos, 22, 173-190.

Matveev, S., and Ballhaus, C. (2002) Role of water in the origin of podiform chromitite deposits. Earth and Planetary Science Letters, 203, 235-243.

McElduff, B., and Stumpfl, E.F. (1991) The chromite deposits of the Troodos Complex, Cyprus-evidence for the role of a fluid phase accompanying chromite formation. Mineralium Deposita, 26, 307-318.

Melcher, F., Grum, W., Simon, G., Thalhammer, T.V., and Stumpfl, E.F. (1997) Petrogenesis of the ophiolitic giant chromite deposits of Kempirsai, Kazakhstan: a study of solid and fluid inclusions in chromite. Journal of Petrology, 38, 1419-1458.

Mellini, M., Rumori, C., and Viti, C. (2005) Hydrothermally reset magmatic spinels in retrograde serpentinites: formation of 'ferritchromit' rims and chlorite aureoles. Contributions to Mineralogy and Petrology, 149, 266-275.

Nozaka, T. (2005) Metamorphic history of serpentinite mylonites from the Happo ultramafic complex, central Japan. Journal of Metamorphic Geology, 23, 711-723.

Nozaka, T. (2014) Metasomatic hydration of the Oeyama forearc peridotites: Tectonic implications. Lithos, 184, 346-360.

Pagé, P., and Barnes, S.J. (2009) Using trace elements in chromites to constrain the origin of podiform chromitites in the Thetford Mines ophiolite, Quebec, Canada. Economic Geology, 104, 997-1018.

Parlak, O. (2016) The Tauride ophiolites of Anatolia (Turkey): A review. Journal of Earth Science, 27, 901-934.

Passchier, C.W., and Trouw, R.A.J. (2005) Microtectonics. 2nd edition. Springer, Berlin Heidelberg, New York.

Pearce, J.A., Lippard, S.J., and Roberts, S. (1984) Characteristics and tectonics significance of supra-subduction zone ophiolites. Geological Society of London Special Publications, 16, 77-94.

Penniston-Dorland, S.C., Bebout, G.E., von Strandmann, P.A.P., Elliott, T., and Sorensen, S.S. (2012) Lithium and its isotopes as tracers of subduction zone fluids and metasomatic processes: Evidence from the Catalina Schist, California, USA. Geochimica et Cosmochimica Acta, 77, 530-545.

Prichard, H.M., Barnes, S.J., and Godel, B. (2018) A mechanism for chromite growth in

Always consult and cite the final, published document. See http:/www.minsocam.org or GeoscienceWorld

ophiolite complexes: evidence from 3D high-resolution X-ray computed tomography images of chromite grains in Harold's Grave chromitite in the Shetland ophiolite. Mineralogical Magazine, 82, 457-470.
Putirka, K. (2016) Amphibole thermometers and barometers for igneous systems and some implications for eruption mechanisms of felsic magmas at arc volcanoes. American Mineralogist, 101, 841-858.
Qiu, T., and Zhu, Y. (2017) Chromian spinels in highly altered ultramafic rocks from the Sartohay ophiolitic mélange, Xinjiang, NW China. Journal of Asian Earth Sciences, 159, 155-184.
Qiu, T., Yang, J.S., Milushi, I., Wu, W.W., Mekshiqi, N., Xiong, F.H., Zang, C., and Shen, T.T. (2018) Petrology and PGE abundances of high-Cr and high-Al podiform chromitites and peridotites from the Bulqiza Ultramafic Massif, Eastern Mirdita Ophiolite, Albania. Acta Geologica Sinica-English Edition, 92, 1063-1081.
Rassios, A., and Smith, A.G. (2000) Constraints on the formation and emplacement age of western Greek ophiolites (Vourinos, Pindos, and Othris) inferred from deformation structures in peridotites. Special Papers-Geological Society of America, 473-484.
Ridolfi, F., Zanetti, A., Renzulli, A., Perugini, D., Holtz, F., and Oberti, R. (2018) AMFORM, a new mass-based model for the calculation of the unit formula of amphiboles from electron microprobe analyses. American Mineralogist, 103, 1112-1125.
Robertson, A.H.F. (2002) Overview of the genesis and emplacement of Mesozoic ophiolites in the Eastern Mediterranean Tethyan region. Lithos, 65, 1-67.
Rollinson, H. (2008) The geochemistry of mantle chromitites from the northern part of the Oman ophiolite: inferred parental melt compositions. Contributions to Mineralogy and Petrology, 156, 273-288.
Rollinson, H., and Adetunji, J. (2015) The geochemistry and oxidation state of podiform chromitites from the mantle section of the Oman ophiolite: a review. Gondwana Research, 27, 543-554.
Rollinson, H., Mameri, L., and Barry, T. (2018) Polymineralic inclusions in mantle chromitites from the Oman ophiolite indicate a highly magnesian parental melt. Lithos, 310, 381-391.
Rospabé, M., Ceuleneer, G., Benoit, M., Abily, B., and Pinet, P. (2017) Origin of the dunitic mantle-crust transition zone in the Oman ophiolite: The interplay between percolating magmas and high-temperature hydrous fluids. Geology, 45, 471-474.
Sachan, H.K., Mukherjee, B.K., and Bodnar, R.J. (2007) Preservation of methane generated during serpentinization of upper mantle rocks: Evidence from fluid inclusions in the Nidar ophiolite, Indus Suture Zone, Ladakh (India). Earth and Planetary Science Letters, 257, 47-59.
Satsukawa, T., Piazolo, S., González-Jiménez, J.M., Colás, V., Griffin, W.L., O'Reilly, S.Y., Gervilla, F., Fanlo, I., and Kerestedjian. T.N. (2015) Fluid-present deformation

Always consult and cite the final, published document. See http:/www.minsocam.org or GeoscienceWorld

aids chemical modification of chromite: insights from chromites from Golyamo Kamenyane, SE bulgaria. Lithos, 228-229, 78-89.

Schiano, P., Clocchiatti, R., Lorand, J.P., Massare, D., Deloule, E., and Chaussidon, M. (1997) Primitive basaltic melts included in podiform chromites from the Oman ophiolite. Earth and Planetary Science Letters, 146, 489-497.

Slovenec, D., and Šegvić, B. (2018) The first record of ultramafic cumulates from the Mt. Kalnik ophiolite mélange in the SW part of the Zagorje-Mid-Transdanubian Zone (NW Croatia): mineralogy, petrology, geochemistry and tectono-magmatic affinity. Geologia Croatica, 71, 185-197.

Sobolev, A.V., and Chaussidon, M. (1996) H_2O concentrations in primary melts from supra-subduction zones and mid-ocean ridges: Implications for H_2O storage and recycling in the mantle. Earth and Planetary Science Letters, 137, 45-55.

Soret, M., Agard, P., Dubacq, B., Plunder, A., and Yamato, P. (2017) Petrological evidence for stepwise accretion of metamorphic soles during subduction infancy (Semail ophiolite, Oman and UAE). Journal of Metamorphic Geology, 35, 1051-1080.

Spry, A. (1969) Metamorphic Textures. Pergamon Press, New York, 350.

Su, B.X., Zhou, M.F., Jing, J.J., Robinson, P.T., Chen, C., Xiao, Y., Liu, X., Shi, R.D., Lenaz, D., and Hu, Y. (2019) Distinctive melt activity and chromite mineralization in Luobusa and Purang ophiolites, southern Tibet: constraints from trace element compositions of chromite and olivine. Science Bulletin, 64, 108-121.

Su, B.X., Robinson, P.T., Chen, C., Xiao, Y., Melcher, F., Bai, Y., Gu, X.Y., Uysal, I., and Lenaz, D. (2020) The occurrence, origin and fate of water in chromitites in ophiolites. American Mineralogist, 105, 894-903.

Su, B.X., Liu, X., Chen, C., Robinson, P.T., Xiao, Y., Zhou, M.F., Bai, Y., Uysal, I., and Zhang, P.F. (2021). A new model for chromitite formation in ophiolites: Fluid immiscibility. Science China Earth Sciences, doi.org/10.1007/s11430-020-9690-4.

Takahashi, E., Uto, K., and Schilling, J.G. (1987) Primary magma compositions and Mg/Fe ratios of their mantle residues along Mid Atlantic Ridge 29°N to 73°N. Technical Report of Institute of Studies on the Earth's Interior Series A, 9, 1-14.

Uysal, I., Sadiklar, M.B., Tarkian, M., Karsli, O., and Aydin, F. (2005) Mineralogy and composition of the chromitites and their platinum-group minerals from Ortaca (Muğla-SW Turkey): evidence for ophiolitic chromitite genesis. Mineralogy and Petrology, 83, 219-242.

Uysal, I., Tarkian, M., Sadiklar, M.B., Zaccarini, F., Meisel, T., Garuti, G., and Heidrich, S. (2009) Petrology of Al-and Cr-rich ophiolitic chromitites from the Muğla, SW Turkey: implications from composition of chromite, solid inclusions of platinum-group mineral, silicate, and base-metal mineral, and Os-isotope geochemistry. Contributions to Mineralogy and Petrology, 158, 659-674.

Uysal, I., Ersoy, E.Y., Karslı, O., Dilek, Y., Sadıklar, M.B., Ottley, C.J., Tiepolo, M., and Meisel, T. (2012) Coexistence of abyssal and ultra-depleted SSZ type mantle

Always consult and cite the final, published document. See http:/www.minsocam.org or GeoscienceWorld

This is the peer-reviewed, final accepted version for American Mineralogist, published by the Mineralogical Society of America.
The published version is subject to change. Cite as Authors (Year) Title. American Mineralogist, in press.
DOI: https://doi.org/10.2138/am-2021-7593. http://www.minsocam.org/

peridotites in a Neo-Tethyan ophiolite in SW Turkey: Constraints from mineral composition, whole-rock geochemistry (major-trace-REE-PGE), and Re-Os isotope systematics. Lithos, 132, 50-69.

Uysal, I., Akmaz, R.M., Saka, S., and Kapsiotis, A. (2016) Coexistence of compositionally heterogeneous chromitites in the Antalya-Isparta ophiolitic suite, SW Turkey: a record of sequential magmatic processes in the sub-arc lithospheric mantle. Lithos, 248-251, 160-174.

Vukmanovic, Z., Barnes, S.J., Reddy, S.M., Godel, B., and Fiorentini, M.L. (2013) Morphology and microstructure of chromite crystals in chromitites from the Merensky Reef (Bushveld Complex, South Africa). Contributions to Mineralogy and Petrology, 165, 1031-1050.

Wells, P.R.A. (1977) Pyroxene thermometry in simple and complex systems. Contributions to Mineralogy and Petrology, 62, 129-139.

Wojtulek, P.M., Schulz, B., Delura, K., and Dajek, M. (2019) Formation of chromitites and ferrogabbros in ultramafic and mafic members of the Variscan Ślęża ophiolite (SW Poland). Ore Geology Reviews, 106, 97-112.

Xiong, F.H., Yang, J.S., Xu, X.Z., Kapsiotis, A., Hao, X.L., and Liu, Z. (2018a) Compositional and isotopic heterogeneities in the Neo-Tethyan upper mantle recorded by coexisting Al-rich and Cr-rich chromitites in the Purang peridotite massif, SW Tibet (China). Journal of Asian Earth Sciences, 159, 109-129.

Xiong, F.H., Yang, J.S., Dilek, Y., Wang, C.L., Hao, X.L., Xu, X.Z., and Lian, D.Y. (2018b) Petrology and geochemistry of the high-Cr podiform chromitites of the Köycegiz ophiolite, southwest Turkey: implications for the multi-stage evolution of the oceanic upper mantle. Mineralogy and Petrology, 112, 685-704.

Zhou, M.F., Robinson, P.T., and Bai, W.J. (1994) Formation of podiform chromites by melt-rock interaction in the upper mantle. Mineralium Deposita, 29, 98-101.

Zhou, M.F., Robinson, P.T., Su, B.X., Gao, J.F., Li, J.W., Yang, J.S., and Malpas, J. (2014) Compositions of chromite, associated minerals, and parental magmas of podiform chromite deposits: the role of slab contamination of asthenospheric melts in suprasubduction zone environments. Gondwana Research, 26, 262-283.

Always consult and cite the final, published document. See http:/www.minsocam.org or GeoscienceWorld

FIGURE CAPTIONS

Fig. 1. (a) Distribution of major ophiolites in Turkey (after Chen et al., 2018); (b, c) Simplified geological map of the Lycian ophiolite (after GDMRE, 2002); (d) Tectonostratigraphy of the Lycian ophiolitic units (after Parlak, 2016).

Fig. 2. Scanned photographs of thin-sections and back-scattered electron images of the amphibole-bearing chromitites (a-h) and dunites (i-l) from the Lycian ophiolite. Amphibole commonly occurs along the grain boundaries of chromite (b, c, d, f, g); Amphibole occurs as monophase or multiphase assemblages with clinopyroxene in chromite (h). Interstitial amphibole (j), amphibole intergrowth with clinopyroxene (k) and a large amphibole grain in dunite (l). Mineral abbreviation: Amp, amphibole; Chr, chromite; Cpx, clinopyroxene; Ol, olivine; Srp, serpentine.

Fig. 3. Scanned photographs of thin-section and back-scattered electron images of the amphibole-bearing harzburgites from the Lycian ophiolite (a-l). Anhedral amphibole surrounding orthopyroxene (b) or clinopyroxene (c, g, k); Amphibole occurring as discrete grains between adjacent minerals (d, f, j); Amphibole occurring as monophase or multiphase inclusions with clinopyroxene or orthopyroxene in chromite grains (h, l). Mineral abbreviation: Amp, amphibole; Chr, chromite; Cpx, clinopyroxene; Ol, olivine; Opx, orthopyroxene; Srp, serpentine.

Always consult and cite the final, published document. See http:/www.minsocam.org or GeoscienceWorld

This is the peer-reviewed, final accepted version for American Mineralogist, published by the Mineralogical Society of America.
The published version is subject to change. Cite as Authors (Year) Title. American Mineralogist, in press.
DOI: https://doi.org/10.2138/am-2021-7593. http://www.minsocam.org/

Fig. 4. Compositions of minerals in the amphibole-bearing chromitites, dunites and harzburgites of the Lycian ophiolite. The dark grey and dark red squares represent chemical compositions of minerals in the harzburgites and chromitites, respectively (Aldanmaz et al., 2009; Uysal et al., 2005, 2009, 2012; Xiong et al., 2018b). The fields of olivine mantle array and fore-arc peridotite in Fig. 4a are from Takahashi et al. (1987) and Ishii (1992), respectively. The fields of abyssal peridotite and fore-arc peridotite in Fig. 4c are from Liu, T et al. (2019). Fields for high-Cr and high-Al chromite are from Zhou et al. (2014).

Fig. 5. Classification of amphibole in chromitites, dunites and harzburgites of the Lycian ophiolite. The amphibole classification diagram is after Leake et al. (1997).

Fig. 6. Compositional variations of amphibole in the chromitites, dunites and harzburgites of the Lycian ophiolite. The gray squares and triangles in Fig. 6a-f represent interstitial amphibole (Rollinson, 2008) and amphibole inclusions, respectively (Uysal et al., 2009; Borisova et al., 2012; Huang et al., 2017; Liu et al., 2017; Qiu et al., 2018; Xiong et al., 2018b; Wojtulek et al., 2019). The fields of I-Amp (intraplate amphibole) and S-Amp (suprasubduction amphibole) in mantle xenoliths are from Coltorti et al. (2007). The fields of hydrothermal Amp, Amp in DTZ (the dunitic transition zone) and Amp inclusion in chromite of the DTZ are from Rospabé et al. (2017). Data for amphibole in ophiolitic peridotite, shown in dotted line, are from Liu et al. (2010), Khedr

Always consult and cite the final, published document. See http:/www.minsocam.org or GeoscienceWorld

et al. (2014), Çelik et al. (2018) and Slovenec and Šegvić. (2018).

Fig. 7. (a) Field relations among harzburgite, dunite and chromitite of the Lycian ophiolite. Note the lack of strong shearing in any of the rocks; (b, c) back-scattered electron images of the disseminated and nodular chromitites from the ophiolite.

Fig. 8. Crystallization temperatures for both interstitial amphibole and amphibole inclusions in chromite of the Lycian chromitites, dunites and harzburgites estimated using the geothermometer of Putirka (2016). The dark grey diamond and light grey circles represent pyroxene temperature (Wells, 1977) and olivine-chromite exchange temperature (Ballhaus et al., 1991), respectively.

Fig. 9. Correlation diagrams of interstitial amphibole Mg# with clinopyroxene Mg# (a), orthopyroxene Mg# (b) and olivine Fo (c) for the chromitites, dunites and harzburgites in the Lycian ophiolite. The solid lines and dashed lines represent functions of $Y = X$ and $Y = X \pm 1$, respectively.

Fig. 10. A cartoon model showing infiltration of hydrous fluids released from chromite grains in chromitite into the surrounding dunite and harzburgite.

Always consult and cite the final, published document. See http:/www.minsocam.org or GeoscienceWorld

This is the peer-reviewed, final accepted version for American Mineralogist, published by the Mineralogical Society of America.
The published version is subject to change. Cite as Authors (Year) Title. American Mineralogist, in press.
DOI: https://doi.org/10.2138/am-2021-7593. http://www.minsocam.org/

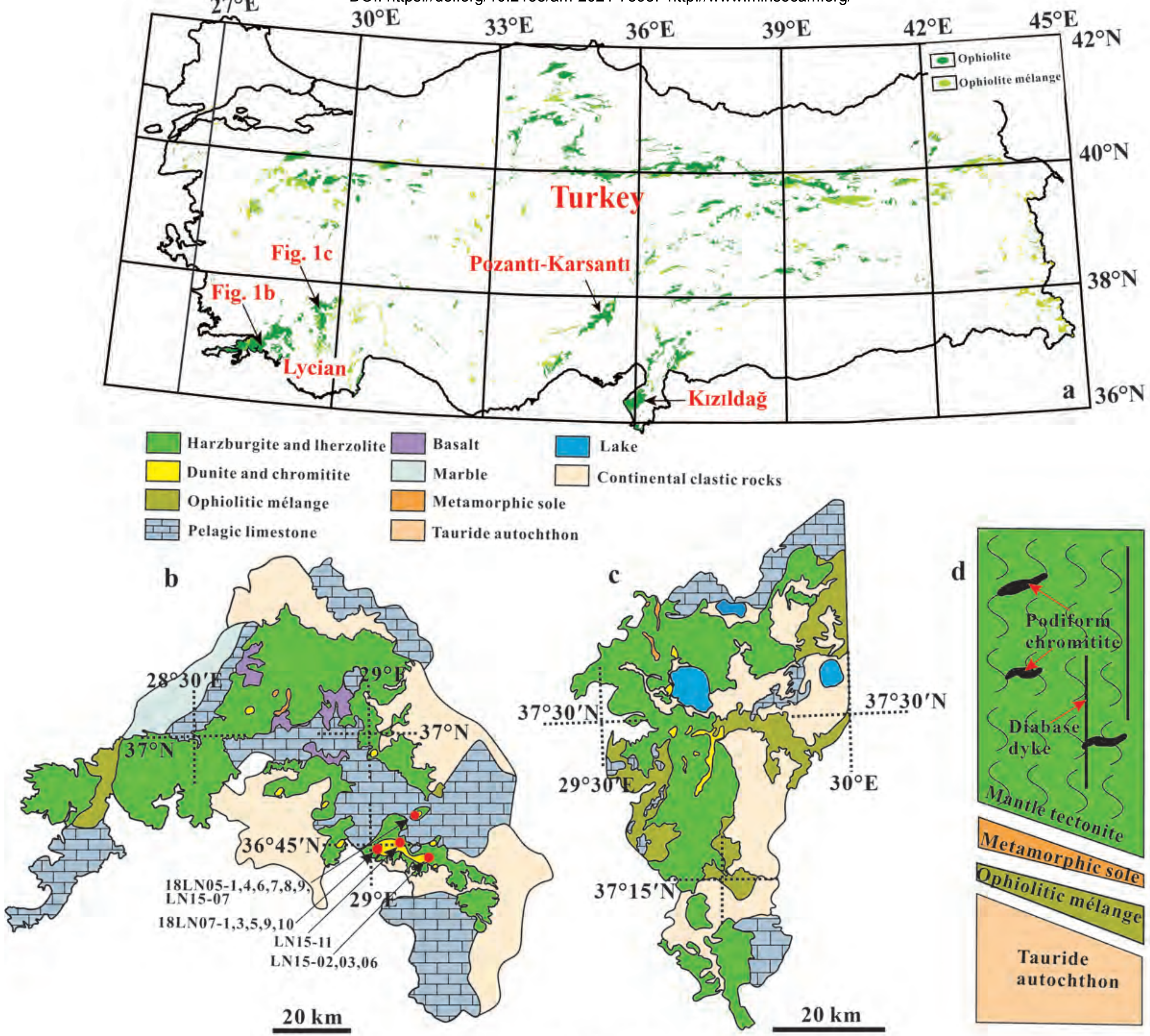

Fig. 1

Always consult and cite the final, published document. See http:/www.minsocam.org or GeoscienceWorld

This is the peer-reviewed, final accepted version for American Mineralogist, published by the Mineralogical Society of America.
The published version is subject to change. Cite as Authors (Year) Title. American Mineralogist, in press.
DOI: https://doi.org/10.2138/am-2021-7593. http://www.minsocam.org/

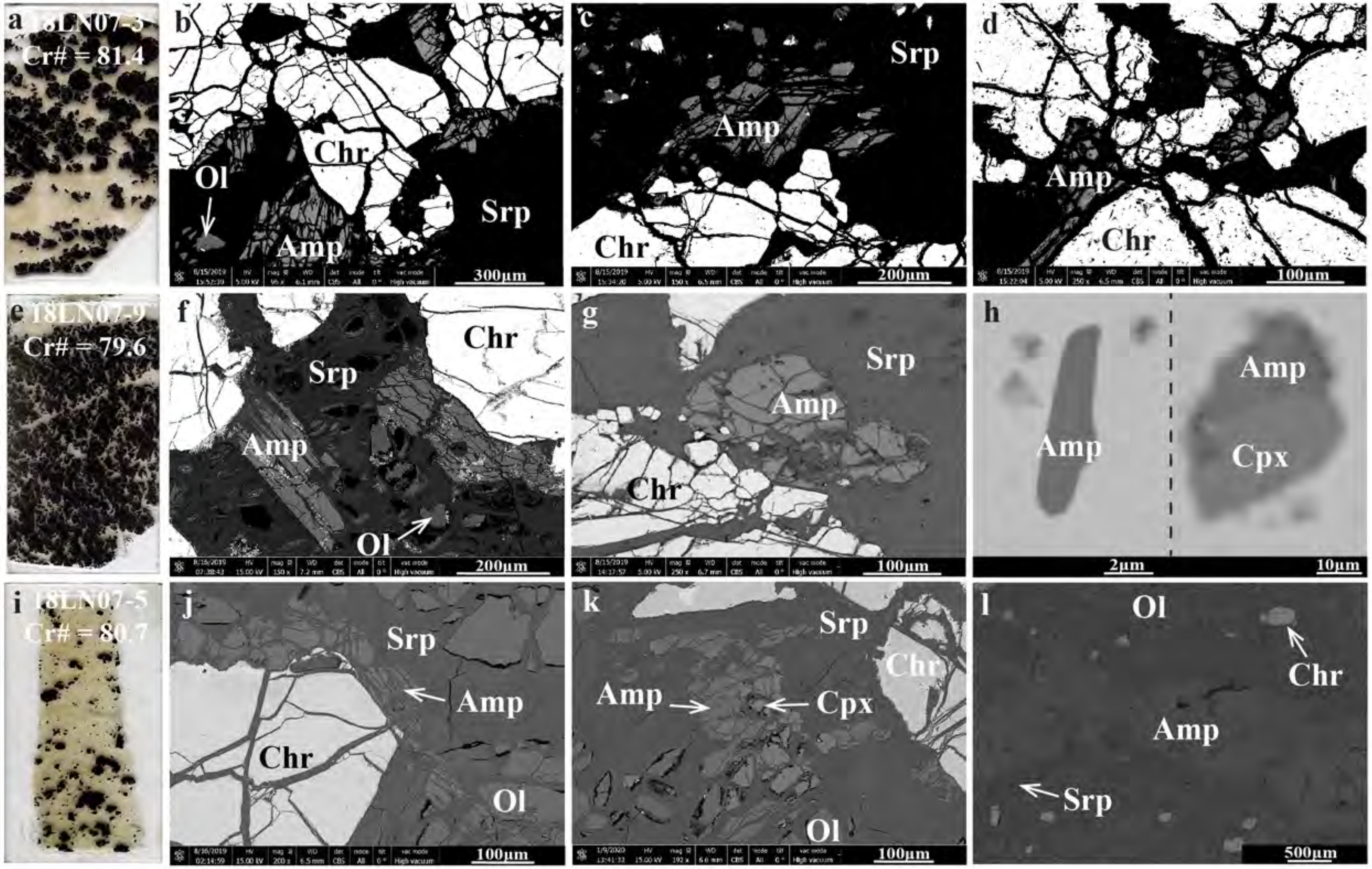

Fig. 2

Always consult and cite the final, published document. See http:/www.minsocam.org or GeoscienceWorld

This is the peer-reviewed, final accepted version for American Mineralogist, published by the Mineralogical Society of America.
The published version is subject to change. Cite as Authors (Year) Title. American Mineralogist, in press.
DOI: https://doi.org/10.2138/am-2021-7593. http://www.minsocam.org/

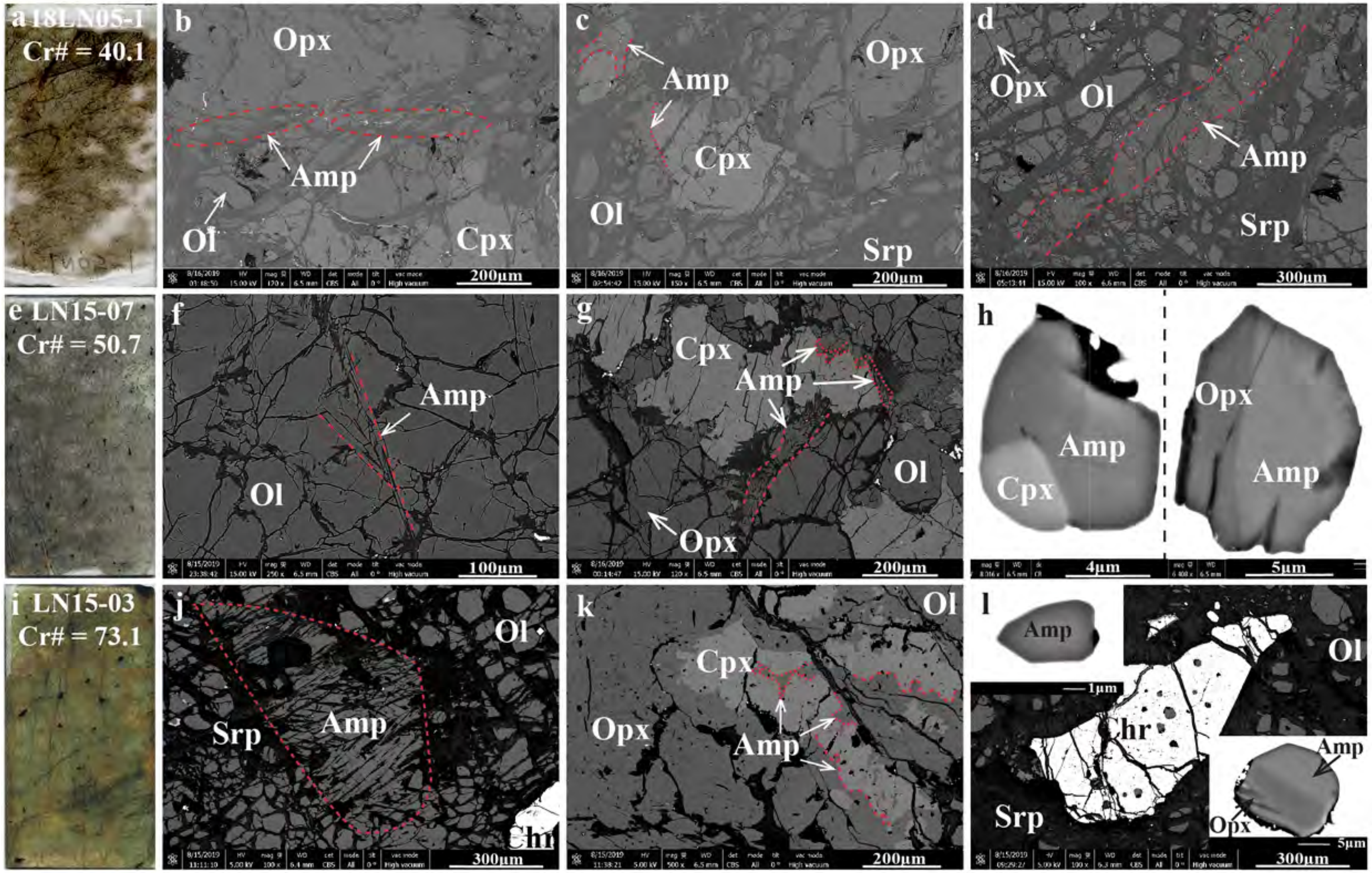

Fig. 3

Always consult and cite the final, published document. See http:/www.minsocam.org or GeoscienceWorld

This is the peer-reviewed, final accepted version for American Mineralogist, published by the Mineralogical Society of America.
The published version is subject to change. Cite as Authors (Year) Title. American Mineralogist, in press.
DOI: https://doi.org/10.2138/am-2021-7593. http://www.minsocam.org/

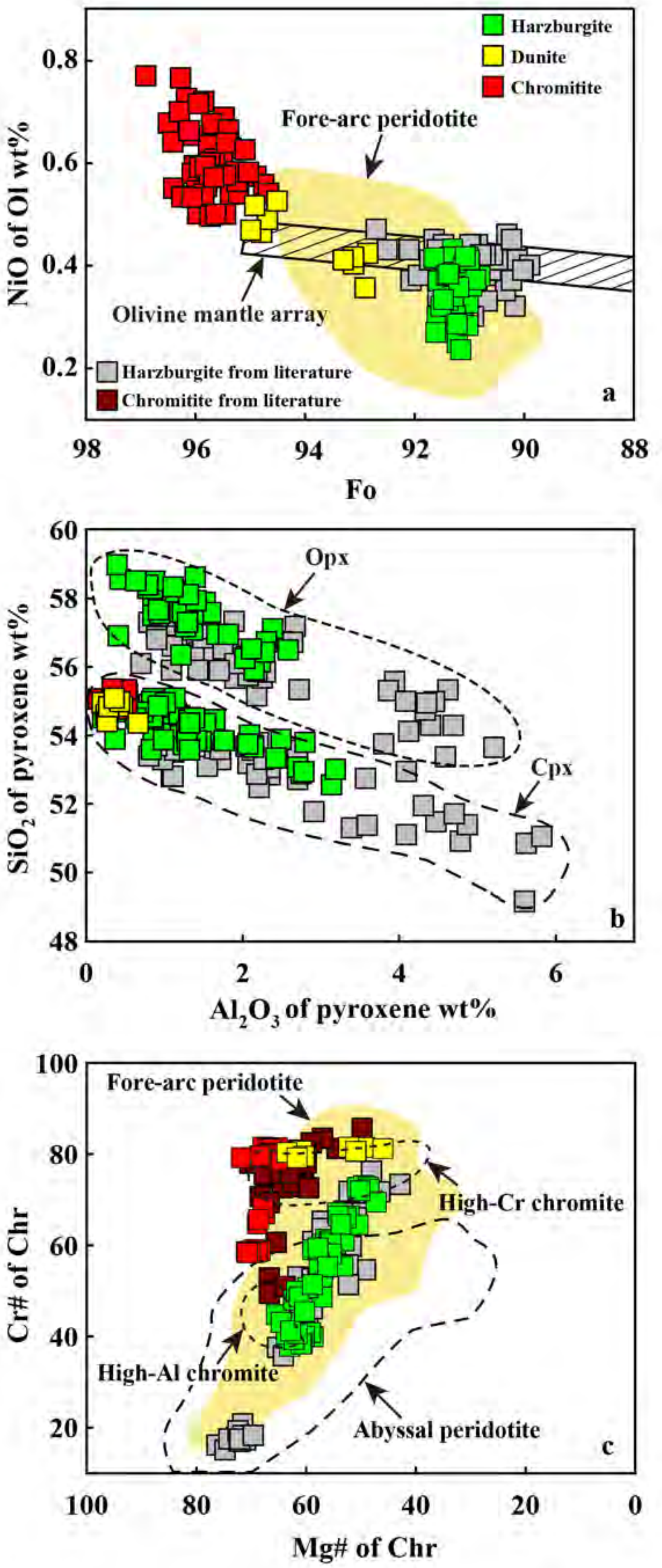

Fig. 4

Always consult and cite the final, published document. See http:/www.minsocam.org or GeoscienceWorld

This is the peer-reviewed, final accepted version for American Mineralogist, published by the Mineralogical Society of America.
The published version is subject to change. Cite as Authors (Year) Title. American Mineralogist, in press.
DOI: https://doi.org/10.2138/am-2021-7593. http://www.minsocam.org/

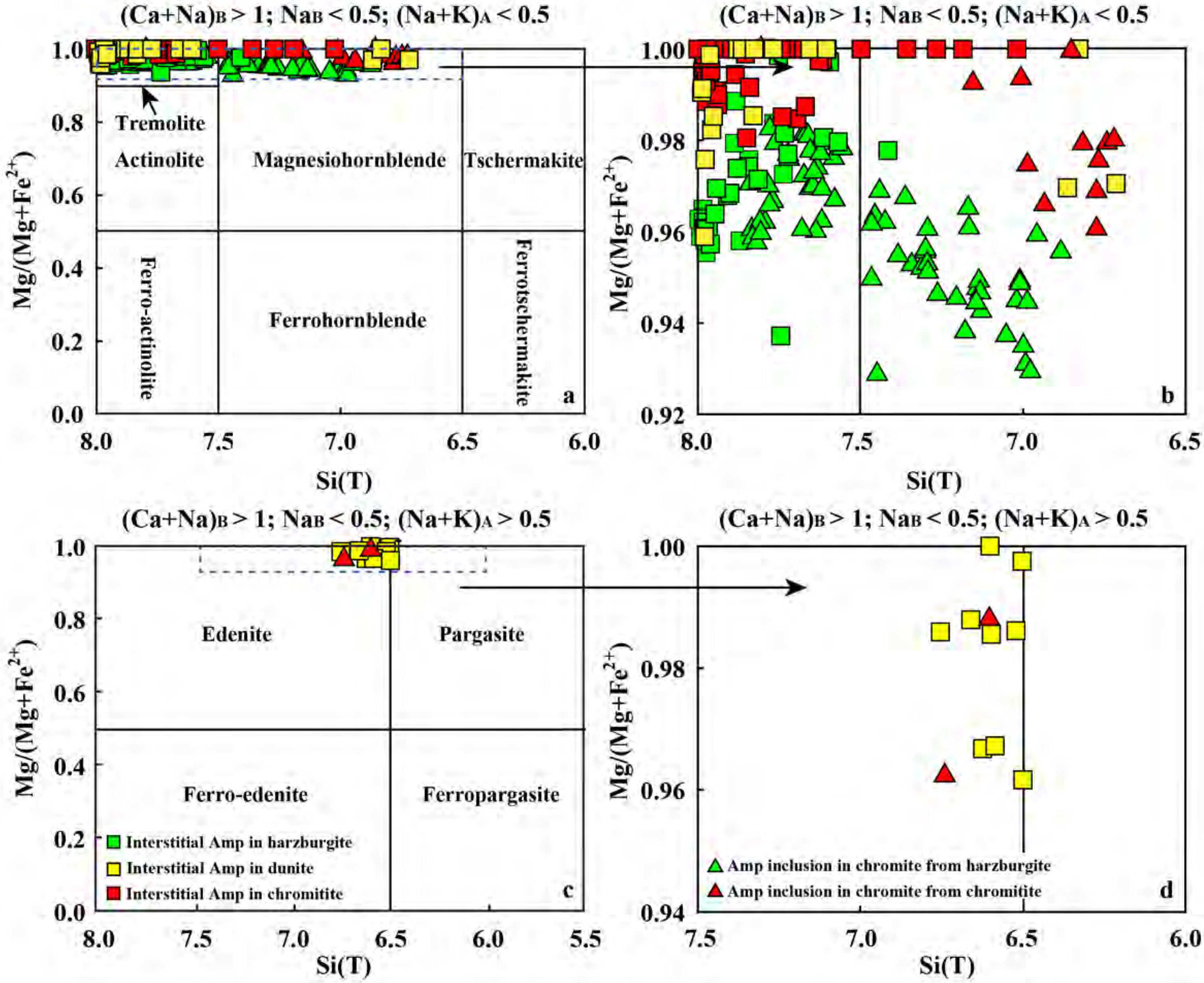

Fig. 5

Always consult and cite the final, published document. See http:/www.minsocam.org or GeoscienceWorld

This is the peer-reviewed, final accepted version for American Mineralogist, published by the Mineralogical Society of America.
The published version is subject to change. Cite as Authors (Year) Title. American Mineralogist, in press.
DOI: https://doi.org/10.2138/am-2021-7593. http://www.minsocam.org/

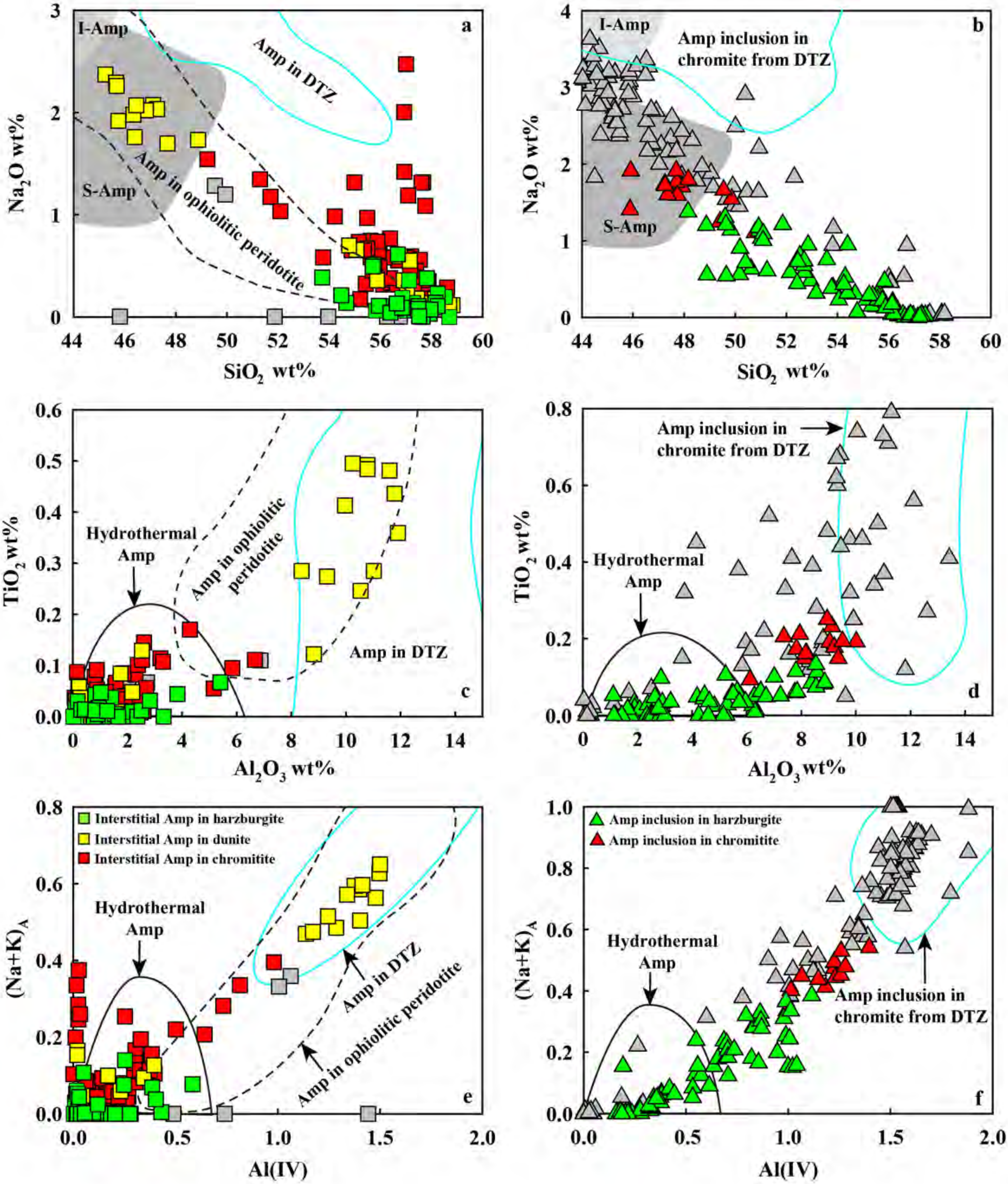

Fig. 6

Always consult and cite the final, published document. See http:/www.minsocam.org or GeoscienceWorld

This is the peer-reviewed, final accepted version for American Mineralogist, published by the Mineralogical Society of America.
The published version is subject to change. Cite as Authors (Year) Title. American Mineralogist, in press.
DOI: https://doi.org/10.2138/am-2021-7593. http://www.minsocam.org/

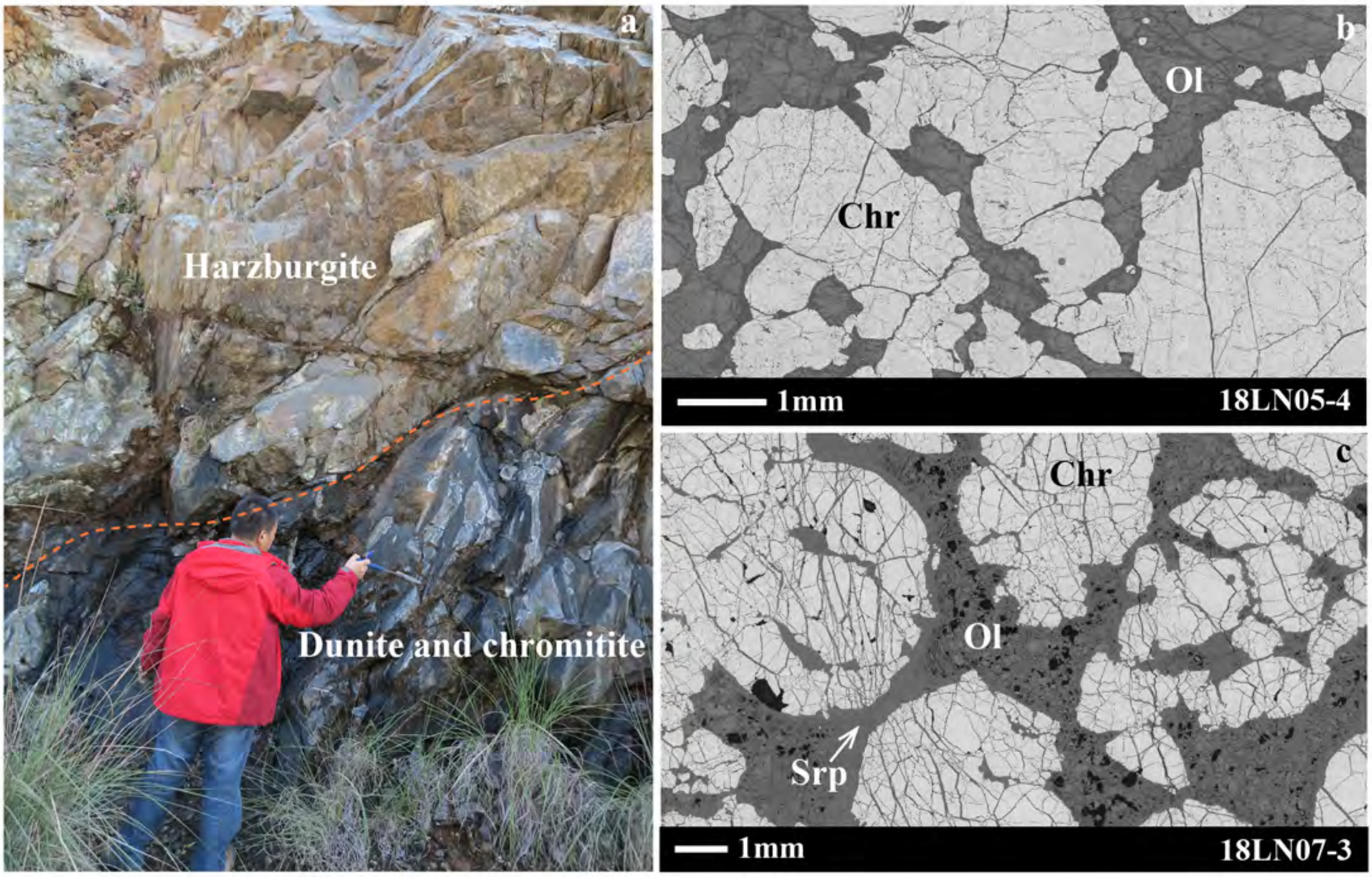

Fig. 7

Always consult and cite the final, published document. See http:/www.minsocam.org or GeoscienceWorld

This is the peer-reviewed, final accepted version for American Mineralogist, published by the Mineralogical Society of America.
The published version is subject to change. Cite as Authors (Year) Title. American Mineralogist, in press.
DOI: https://doi.org/10.2138/am-2021-7593. http://www.minsocam.org/

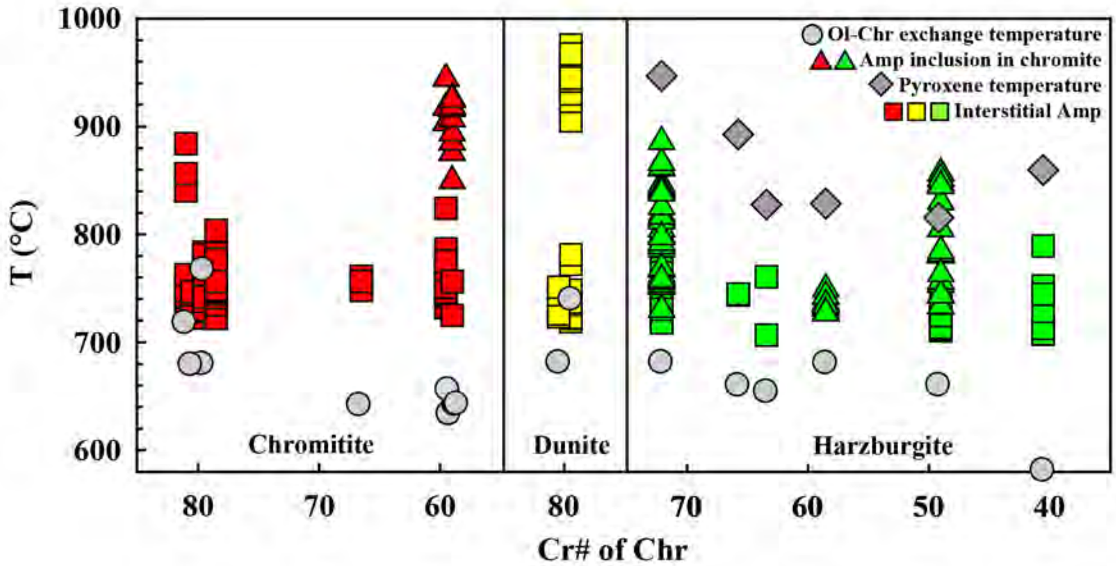

Fig. 8

Always consult and cite the final, published document. See http:/www.minsocam.org or GeoscienceWorld

This is the peer-reviewed, final accepted version for American Mineralogist, published by the Mineralogical Society of America.
The published version is subject to change. Cite as Authors (Year) Title. American Mineralogist, in press.
DOI: https://doi.org/10.2138/am-2021-7593. http://www.minsocam.org/

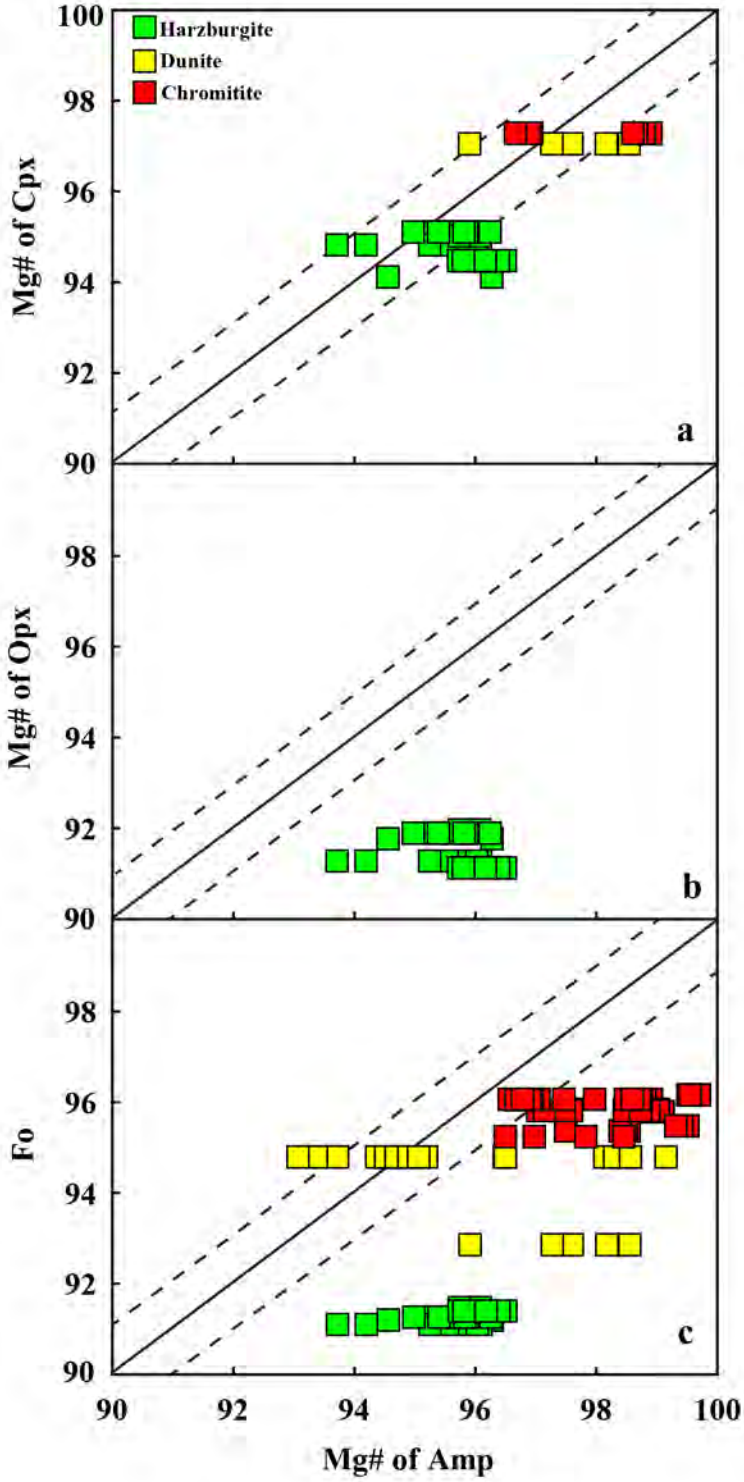

Fig. 9

Always consult and cite the final, published document. See http:/www.minsocam.org or GeoscienceWorld

This is the peer-reviewed, final accepted version for American Mineralogist, published by the Mineralogical Society of America.
The published version is subject to change. Cite as Authors (Year) Title. American Mineralogist, in press.
DOI: https://doi.org/10.2138/am-2021-7593. http://www.minsocam.org/

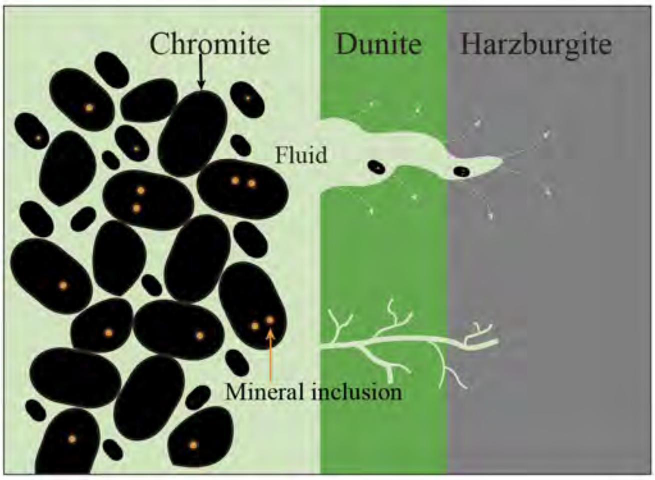

Fig. 10

Always consult and cite the final, published document. See http:/www.minsocam.org or GeoscienceWorld

DOI: https://doi.org/10.2138/am-2021-7593. http://www.minsocam.org/

Table 1. Mineral modal abundance (vol.%) of the harzburgite, dunite and chromitite from the Lycian ophiolite.

Sample	Ol	Opx	Cpx	Chr	Amp
Harzburgite					
18LN05-1	85.2	10.4	2.9	0.8	0.7
18LN07-1	84.6	9.6	2.8	1.9	1.1
LN15-02	86.3	9.4	2.8	0.9	0.6
LN15-03	84.5	11.2	1.8	1.6	0.9
LN15-07	84.4	10.5	2.8	1.5	0.8
LN15-11	85.3	10.3	2.7	0.9	0.8
Dunite					
18LN07-5	77.4	0	0.9	19.9	1.8
LN15-06	92.3	0	0.8	5.3	1.6
Chromitite					
18LN05-4	33.5	0	0	65.3	1.2
18LN05-6	30.3	0	0	68.3	1.4
18LN05-7	27.3	0	0	71.3	1.4
18LN05-8	23.4	0	0	75.0	1.6
18LN05-9	18.3	0	0	79.9	1.8
18LN07-3	71.4	0	0.5	27.0	1.1
18LN07-9-1	40.6	0	0	58.1	1.3
18LN07-9-2	36.4	0	0	62.4	1.2
18LN07-10	78.3	0	0.2	20.4	1.1

Note:

Ol: olivine; Opx: orthopyroxene; Cpx: clinopyroxene; Chr: chromite; Amp: amphibole.

This is the peer-reviewed, final accepted version for American Mineralogist, published by the Mineralogical Society of America.
The published version is subject to change. Cite as Authors (Year) Title. American Mineralogist, in press.
DOI: https://doi.org/10.2138/am-2021-7593. http://www.minsocam.org/

Table 2. Representative major element compositions (wt%) of olivine, clinopyroxene, orthopyroxene and chromite in the harzburgite, dunite and chromitite from the Lycian ophiolite.

Sample	18LN05-1					18LN07-1							LN15-02					LN15-03				
Rock	Harzburgite					Harzburgite							Harzburgite					Harzburgite				
Mineral	Ol	Ol[1]	Cpx	Opx	Chr	Ol	Ol[1]	Cpx	Cpx[1]	Opx	Opx[1]	Chr	Ol	Ol[1]	Cpx	Opx	Chr	Ol	Ol[1]	Cpx	Cpx[1]	Opx
SiO_2	41.3	41.7	54.2	57.1	b.d.l.	41.6	40.6	54.0	54.3	57.9	57.4	b.d.l.	41.3	41.5	54.3	57.3	b.d.l.	40.7	40.9	53.9	53.9	57.5
TiO_2	b.d.l.	0.01	b.d.l.	0.03	0.04	0.01	b.d.l.	0.03	b.d.l.	0.01	0.02	0.07	0.01	0.03	0.03	b.d.l.	0.03	b.d.l.	b.d.l.	0.01	b.d.l.	0.04
Al_2O_3	b.d.l.	0.03	1.52	2.38	34.2	b.d.l.	b.d.l.	1.58	1.01	1.52	1.11	21.3	b.d.l.	0.04	1.05	1.26	17.7	0.01	0.01	0.86	0.67	0.92
Cr_2O_3	0.07	0.76	0.43	0.65	34.2	b.d.l.	0.32	0.72	1.12	0.66	0.57	47.9	0.03	0.64	0.36	0.53	52.1	b.d.l.	1.08	0.47	1.27	0.47
FeO	8.73	8.42	1.78	5.65	17.1	8.44	7.91	1.92	1.82	5.64	5.62	17.8	8.33	8.26	1.70	5.30	19.2	8.61	6.28	1.66	1.83	5.39
MnO	0.13	0.12	0.06	0.08	0.20	0.11	0.05	0.09	0.02	0.13	0.10	0.32	0.06	0.15	0.02	0.12	0.04	0.06	0.05	0.04	0.07	0.17
MgO	49.5	49.4	18.0	32.7	14.2	49.4	50.4	17.3	18.0	34.3	35.3	12.2	49.5	48.8	18.0	33.5	11.0	49.8	51.4	17.8	17.7	33.7
CaO	0.02	0.02	24.2	0.74	b.d.l.	0.04	b.d.l.	23.9	24.3	0.75	0.30	0.02	0.04	0.02	24.5	1.19	0.02	b.d.l.	b.d.l.	24.4	23.9	1.32
Na_2O	0.01	0.07	0.06	0.04	0.05	b.d.l.	b.d.l.	0.03	0.07	b.d.l.	b.d.l.	b.d.l.	0.01	b.d.l.	0.02	b.d.l.	0.01	0.02	b.d.l.	0.02	0.11	b.d.l.
K_2O	0.03	0.02	b.d.l.	b.d.l.	0.01	b.d.l.	b.d.l.	0.03	0.01	b.d.l.	b.d.l.	b.d.l.	0.01	b.d.l.	b.d.l.	0.01	b.d.l.	0.01	b.d.l.	b.d.l.	b.d.l.	0.01
NiO	0.38	0.36	0.05	0.05	0.02	0.41	0.31	0.03	0.05	0.06	0.09	0.06	0.34	0.27	0.04	0.06	0.02	0.27	0.33	0.04	0.03	0.09
Total	100	101	100	99.4	99.9	100	99.5	99.7	101	101	100	99.7	99.6	99.7	99.9	99.3	100	99.5	100	99.2	99.5	99.6
Si	1.006	1.008	1.958	1.974	0.000	1.012	0.993	1.965	1.960	1.973	1.965	0.000	1.009	1.012	1.970	1.985	0.000	0.998	0.990	1.972	1.968	1.987
Ti	0.000	0.000	0.000	0.001	0.001	0.000	0.000	0.001	0.000	0.000	0.001	0.002	0.000	0.001	0.001	0.000	0.001	0.000	0.000	0.000	0.000	0.001
Al	0.000	0.001	0.065	0.097	1.174	0.000	0.000	0.068	0.043	0.061	0.045	0.780	0.000	0.001	0.045	0.051	0.660	0.000	0.000	0.037	0.029	0.037
Cr	0.001	0.014	0.012	0.018	0.787	0.000	0.006	0.021	0.032	0.018	0.015	1.179	0.001	0.012	0.010	0.014	1.306	0.000	0.021	0.014	0.037	0.013
Fe^{2+}	0.178	0.170	0.054	0.163	0.375	0.172	0.162	0.058	0.055	0.161	0.161	0.426	0.170	0.169	0.052	0.153	0.476	0.177	0.127	0.051	0.056	0.156
Fe^{3+}					0.040							0.038					0.033					
Mn	0.003	0.003	0.002	0.002	0.005	0.002	0.001	0.003	0.001	0.004	0.003	0.008	0.001	0.003	0.001	0.003	0.001	0.001	0.001	0.001	0.002	0.005
Mg	1.796	1.779	0.972	1.683	0.616	1.793	1.836	0.940	0.970	1.742	1.800	0.565	1.801	1.777	0.971	1.727	0.518	1.820	1.855	0.971	0.965	1.737
Ca	0.000	0.001	0.937	0.027	0.000	0.001	0.000	0.931	0.939	0.027	0.011	0.001	0.001	0.001	0.951	0.044	0.001	0.000	0.000	0.956	0.938	0.049
Na	0.001	0.003	0.004	0.003	0.001	0.000	0.000	0.002	0.005	0.000	0.000	0.000	0.000	0.000	0.002	0.000	0.000	0.001	0.000	0.001	0.007	0.000
K	0.001	0.001	0.000	0.000	0.000	0.000	0.000	0.001	0.001	0.000	0.000	0.000	0.000	0.000	0.000	0.001	0.000	0.000	0.000	0.000	0.000	0.000
Ni	0.008	0.007	0.001	0.001	0.000	0.008	0.006	0.001	0.001	0.002	0.002	0.002	0.007	0.005	0.001	0.002	0.001	0.005	0.006	0.001	0.001	0.002
Total	2.994	2.986	4.005	3.969	3.000	2.988	3.004	3.992	4.006	3.987	4.004	3.000	2.990	2.981	4.002	3.982	2.996	3.003	3.000	4.003	4.003	3.990
Mg#	91.1	91.3	94.8	91.2	62.2	91.3	92.0	94.2	94.7	91.6	91.9	57.0	91.4	91.4	95.0	91.9	52.1	91.2	93.6	95.1	94.6	91.8
Cr#					40.1							60.2					66.4					
T[1](°C)					859							828					892					
T[2](°C)					581							680					660					

This is the peer-reviewed, final accepted version for American Mineralogist, published by the Mineralogical Society of America.
The published version is subject to change. Cite as Authors (Year) Title. American Mineralogist, in press.
DOI: https://doi.org/10.2138/am-2021-7593. http://www.minsocam.org/

(Table 2 continued)

Sample			LN15-07							LN15-11				18LN07-5		LN15-06			18LN05-4		18LN05-6	
Rock			Harzburgite							Harzburgite				Dunite		Dunite			Chromitite		Chromitite	
Mineral	Opx[1]	Chr	Ol	Ol[1]	Cpx	Cpx[1]	Opx	Opx[1]	Chr	Ol	Cpx	Opx	Chr	Ol	Chr	Ol	Cpx	Chr	Ol	Ol[1]	Chr	Ol
SiO_2	57.7	b.d.l.	40.7	40.8	54.4	54.2	56.4	57.1	b.d.l.	40.9	53.8	57.1	b.d.l.	41.4	b.d.l.	41.9	55.0	b.d.l.	41.9	41.6	b.d.l.	41.7
TiO_2	b.d.l.	0.02	b.d.l.	b.d.l.	0.01	0.02	0.01	b.d.l.	0.02	b.d.l.	0.06	b.d.l.	0.02	0.01	0.17	0.02	0.01	0.13	b.d.l.	b.d.l.	0.10	0.02
Al_2O_3	0.29	13.7	b.d.l.	b.d.l.	1.53	1.14	2.28	1.16	28.7	b.d.l.	1.29	1.36	19.2	0.02	9.65	b.d.l.	0.21	9.15	b.d.l.	b.d.l.	22.2	b.d.l.
Cr_2O_3	0.61	55.3	b.d.l.	0.11	0.35	1.03	0.70	1.23	39.4	b.d.l.	0.47	0.48	50.1	0.01	60.0	0.01	0.26	60.1	0.01	0.21	47.5	0.01
FeO	5.41	20.1	8.53	7.48	1.89	1.82	5.81	5.58	16.8	8.56	1.97	5.67	18.9	5.16	17.2	6.94	0.99	19.3	4.56	3.80	14.4	4.75
MnO	0.08	b.d.l.	0.10	0.06	0.05	0.05	0.17	0.08	b.d.l.	0.09	0.10	0.10	b.d.l.	0.07	0.33	0.11	0.02	b.d.l.	0.10	0.03	0.20	0.09
MgO	35.5	10.1	50.2	51.3	17.9	17.8	32.9	35.1	13.8	49.1	17.5	34.9	11.6	51.9	12.5	49.9	18.1	10.5	51.8	54.3	15.5	52.5
CaO	0.21	0.03	b.d.l.	b.d.l.	24.5	24.4	0.90	0.25	0.01	0.03	23.8	0.48	0.03	0.02	b.d.l.	0.03	25.6	0.02	0.02	0.01	b.d.l.	b.d.l.
Na_2O	0.01	b.d.l.	b.d.l.	0.01	0.03	0.06	b.d.l.	b.d.l.	b.d.l.	b.d.l.	b.d.l.	b.d.l.	0.01	b.d.l.	b.d.l.	b.d.l.	0.11	0.02	b.d.l.	b.d.l.	0.10	0.06
K_2O	0.01	0.01	b.d.l.	b.d.l.	b.d.l.	b.d.l.	b.d.l.	0.02	b.d.l.	b.d.l.	0.01	b.d.l.	0.01	0.01	0.02	b.d.l.	b.d.l.	b.d.l.	0.05	b.d.l.	0.03	b.d.l.
NiO	0.06	0.10	0.33	0.34	0.03	0.06	0.11	0.05	0.06	0.36	0.06	0.07	0.05	0.46	0.05	0.42	b.d.l.	0.03	0.54	0.55	0.19	0.56
Total	99.9	99.3	99.9	100	101	101	99.4	101	98.8	99.1	99.1	100	99.9	99.1	100	99.3	100	99.3	99.0	100	100	99.7
Si	1.984	0.003	0.995	0.991	1.960	1.958	1.958	1.957	0.000	1.007	1.970	1.961	0.001	1.004	0.000	1.019	1.988	0.000	1.013	0.990	0.000	1.003
Ti	0.000	0.000	0.000	0.000	0.000	0.000	0.000	0.000	0.000	0.000	0.002	0.000	0.000	0.000	0.004	0.000	0.000	0.003	0.000	0.000	0.002	0.000
Al	0.012	0.525	0.000	0.000	0.065	0.049	0.093	0.047	1.016	0.000	0.056	0.055	0.708	0.000	0.370	0.000	0.009	0.358	0.000	0.000	0.790	0.000
Cr	0.016	1.425	0.000	0.002	0.010	0.030	0.019	0.033	0.935	0.000	0.014	0.013	1.241	0.000	1.543	0.000	0.007	1.577	0.000	0.004	1.133	0.000
Fe^{2+}	0.156	0.503	0.174	0.152	0.057	0.055	0.169	0.160	0.375	0.176	0.060	0.163	0.447	0.105	0.389	0.141	0.030	0.476	0.092	0.076	0.285	0.096
Fe^{3+}		0.044							0.048				0.049		0.079			0.059			0.078	
Mn	0.002	0.000	0.002	0.001	0.002	0.001	0.005	0.002	0.000	0.002	0.003	0.003	0.000	0.001	0.009	0.002	0.001	0.000	0.002	0.001	0.005	0.002
Mg	1.823	0.492	1.828	1.855	0.962	0.960	1.704	1.794	0.619	1.801	0.952	1.789	0.544	1.876	0.604	1.810	0.973	0.520	1.868	1.928	0.697	1.884
Ca	0.008	0.001	0.000	0.000	0.945	0.946	0.033	0.009	0.000	0.001	0.935	0.018	0.001	0.001	0.000	0.001	0.992	0.001	0.000	0.000	0.000	0.000
Na	0.001	0.000	0.000	0.000	0.002	0.004	0.000	0.000	0.000	0.000	0.000	0.000	0.000	0.000	0.000	0.000	0.008	0.000	0.000	0.000	0.001	0.003
K	0.000	0.000	0.000	0.000	0.000	0.000	0.000	0.001	0.000	0.000	0.000	0.000	0.000	0.000	0.000	0.000	0.000	0.000	0.001	0.000	0.000	0.000
Ni	0.002	0.003	0.007	0.007	0.001	0.002	0.003	0.001	0.001	0.007	0.002	0.002	0.001	0.009	0.001	0.008	0.000	0.001	0.010	0.010	0.005	0.011
Total	4.003	2.996	3.005	3.008	4.003	4.004	3.985	4.004	2.995	2.993	3.994	4.004	2.992	2.996	3.000	2.981	4.008	2.995	2.988	3.008	2.997	2.998
Mg#	92.2	49.5	91.4	92.5	94.5	94.6	91.1	91.9	62.3	91.2	94.1	91.7	52.5	94.8	60.8	92.8	97.0	52.2	95.3	96.3	66.0	95.2
Cr#		73.1							47.9				63.7		80.7			81.5			59	
T^1(°C)		946							815				827									
T^2(°C)		681							660				654		739			680			633	

This is the peer-reviewed, final accepted version for American Mineralogist, published by the Mineralogical Society of America.
The published version is subject to change. Cite as Authors (Year) Title. American Mineralogist, in press.
DOI: https://doi.org/10.2138/am-2021-7593. http://www.minsocam.org/

(Table 2 continued)

Sample			18LN05-7			18LN05-8			18LN05-9		18LN07-3				18LN07-9-1			18LN07-9-2		18LN07-10			
Rock			Chromitite			Chromitite			Chromitite		Chromitite				Chromitite			Chromitite		Chromitite			
Mineral	Cpx[1]	Chr	Ol	Ol[1]	Chr	Ol	Cpx[1]	Chr	Ol	Chr	Ol	Cpx	Cpx[1]	Chr	Ol	Ol[1]	Chr	Ol	Chr	Ol	Ol[1]	Chr	DL
SiO_2	53.9	b.d.l.	42.3	41.7	b.d.l.	42.0	53.9	b.d.l.	43.0	0.09	42.2	55.3	54.3	b.d.l.	41.3	41.8	b.d.l.	41.4	b.d.l.	43.0	41.1	b.d.l.	0.01
TiO_2	0.03	0.12	b.d.l.	b.d.l.	0.10	0.02	b.d.l.	0.14	b.d.l.	0.15	b.d.l.	0.03	0.04	0.10	b.d.l.	b.d.l.	0.17	b.d.l.	0.15	b.d.l.	0.02	0.20	0.02
Al_2O_3	1.22	22.6	b.d.l.	b.d.l.	21.9	b.d.l.	0.90	22.6	b.d.l.	17.4	b.d.l.	0.52	0.34	9.48	b.d.l.	b.d.l.	10.1	0.02	10.3	b.d.l.	0.01	9.83	0.01
Cr_2O_3	1.14	47.2	b.d.l.	0.19	48.4	b.d.l.	1.07	47.2	0.05	53.1	b.d.l.	0.50	1.13	61.8	b.d.l.	0.25	61.2	0.04	60.2	0.05	0.42	61.2	0.03
FeO	1.33	14.5	4.17	3.74	14.7	4.46	1.28	14.3	3.87	13.4	3.95	0.89	0.70	14.5	4.21	3.00	14.1	3.97	14.5	4.19	2.73	15.5	0.01
MnO	0.02	0.18	0.03	0.04	0.26	0.07	0.01	0.21	0.05	0.27	0.02	0.04	0.03	0.21	0.08	0.02	0.22	0.04	0.26	0.02	0.04	0.30	0.06
MgO	18.1	15.3	53.2	53.9	15.3	52.0	17.8	15.5	53.6	15.9	53.2	17.6	18.2	13.4	53.3	54.7	13.8	53.5	13.7	52.7	54.3	12.7	0.06
CaO	24.4	b.d.l.	0.03	0.03	0.02	0.01	24.4	0.01	0.04	0.01	0.01	24.9	24.1	0.02	0.01	0.02	b.d.l.	0.01	b.d.l.	0.03	0.02	b.d.l.	0.02
Na_2O	0.11	0.02	b.d.l.	b.d.l.	b.d.l.	b.d.l.	0.17	0.01	b.d.l.	0.03	b.d.l.	0.22	0.21	0.01	0.04	0.01	b.d.l.	0.01	0.01	0.02	0.02	b.d.l.	0.03
K_2O	b.d.l.	0.01	b.d.l.	b.d.l.	b.d.l.	b.d.l.	0.01	b.d.l.	0.01	b.d.l.	b.d.l.	0.01	b.d.l.	b.d.l.	0.02	b.d.l.	0.01	b.d.l.	b.d.l.	0.01	0.02	b.d.l.	0.02
NiO	0.03	0.16	0.72	0.58	0.15	0.69	0.06	0.14	0.73	0.15	0.58	0.03	0.02	0.09	0.59	0.78	0.04	0.53	0.13	0.57	0.51	0.02	0.03
Total	100	100	100	100	101	99.2	99.6	100	101	100	100	100	99.1	99.6	99.5	101	99.7	99.5	99.3	101	99.1	99.7	
Si	1.951	0.000	1.008	0.994	0.000	1.013	1.965	0.000	1.012	0.003	1.008	1.999	1.981	0.000	0.994	0.991	0.002	0.996	0.000	1.020	0.988	0.000	
Ti	0.001	0.003	0.000	0.000	0.002	0.000	0.000	0.003	0.000	0.003	0.000	0.001	0.001	0.002	0.000	0.000	0.004	0.000	0.004	0.000	0.000	0.005	
Al	0.052	0.804	0.000	0.000	0.777	0.000	0.039	0.803	0.000	0.628	0.000	0.022	0.014	0.362	0.000	0.000	0.384	0.001	0.394	0.000	0.000	0.377	
Cr	0.033	1.128	0.000	0.004	1.153	0.000	0.031	1.126	0.001	1.286	0.000	0.014	0.033	1.584	0.000	0.005	1.558	0.001	1.540	0.001	0.008	1.574	
Fe^{2+}	0.040	0.303	0.083	0.075	0.305	0.090	0.039	0.297	0.076	0.266	0.079	0.027	0.021	0.345	0.085	0.059	0.334	0.080	0.334	0.083	0.055	0.382	
Fe^{3+}		0.064			0.065			0.065		0.076				0.049			0.046		0.059			0.039	
Mn	0.001	0.005	0.001	0.001	0.007	0.001	0.000	0.005	0.001	0.007	0.000	0.001	0.001	0.006	0.002	0.000	0.006	0.001	0.007	0.000	0.001	0.008	
Mg	0.976	0.689	1.886	1.918	0.687	1.869	0.964	0.696	1.883	0.725	1.893	0.947	0.991	0.647	1.913	1.935	0.665	1.915	0.658	1.863	1.945	0.614	
Ca	0.948	0.000	0.001	0.001	0.001	0.000	0.954	0.000	0.001	0.000	0.000	0.963	0.944	0.001	0.000	0.000	0.000	0.000	0.000	0.001	0.000	0.000	
Na	0.007	0.000	0.000	0.000	0.000	0.000	0.012	0.000	0.000	0.001	0.000	0.015	0.015	0.000	0.002	0.001	0.000	0.000	0.000	0.001	0.001	0.000	
K	0.000	0.000	0.000	0.000	0.000	0.000	0.001	0.000	0.000	0.000	0.000	0.001	0.000	0.000	0.001	0.000	0.000	0.000	0.000	0.000	0.001	0.000	
Ni	0.001	0.004	0.014	0.011	0.004	0.013	0.002	0.003	0.014	0.004	0.011	0.001	0.001	0.002	0.011	0.015	0.001	0.010	0.003	0.011	0.010	0.000	
Total	4.009	2.999	2.992	3.004	3.000	2.987	4.007	3.000	2.988	2.999	2.992	3.990	4.001	3.000	3.007	3.007	3.000	3.004	3.000	2.980	3.009	3.000	
Mg#	96.1	69.5	95.8	96.3	65.2	95.5	96.1	70.1	96.1	68.1	96.0	97.3	97.9	65.2	95.8	97.0	66.5	96.0	66.4	95.8	97.3	59.5	
Cr#		58.4			59.8			58.4		67.2				81.4			80.2		79.6			80.7	
T^1(°C)																							
T^2(°C)		642			655			642		641				717			679		766			678	

Always consult and cite the final, published document. See http:/www.minsocam.org or GeoscienceWorld

This is the peer-reviewed, final accepted version for American Mineralogist, published by the Mineralogical Society of America.
The published version is subject to change. Cite as Authors (Year) Title. American Mineralogist, in press.
DOI: https://doi.org/10.2138/am-2021-7593. http://www.minsocam.org/

Note:

Ol[1]: olivine inclusion in chromite; Cpx[1]: clinopyroxene inclusion in chromite; Opx[1]: orthopyroxene inclusion in chromite; b.d.l.: value below detection limit; DL: detection limit of the oxide; The data in the table represent the average value; a minimum of three grains were analyzed for each mineral phase in a single thin section and at least two points were analyzed in the cores and rims of each crystal.

Mg#: 100Mg / (Mg + Fe^{2+}); Cr#: 100Cr / (Cr + Al).

T[1]: pyroxene temperature (Wells, 1977); T[2]: olivine-chromite exchange temperature (Ballhaus et al., 1991).

Always consult and cite the final, published document. See http:/www.minsocam.org or GeoscienceWorld

This is the peer-reviewed, final accepted version for American Mineralogist, published by the Mineralogical Society of America.
The published version is subject to change. Cite as Authors (Year) Title. American Mineralogist, in press.
DOI: https://doi.org/10.2138/am-2021-7593. http://www.minsocam.org/

Table 3. Major element compositions (wt%) of amphibole in the harzburgite, dunite and chromitite from the Lycian ophiolite.

Sample	18LN05-1							18LN07-1													LN15-02	
Rock	Harzburgite							Harzburgite													Harzburgite	
Mineral	Amp[1]	Amp[1]	Amp[1]	Amp[1]	Amp[1]	Amp[1]	Amp[1]	Amp[3]	Amp[3]	Amp[3]	Amp[3]	Amp[3]	Amp[3]	Amp[3]	Amp[3]	Amp[3]	Amp[3]	Amp[3]	Amp[3]	Amp[3]	Amp[1]	Amp[1]
Type	Mhb	Tr	Tr	Tr	Tr	Tr	Tr	Tr	Tr	Tr	Tr	Tr	Tr	Tr	Tr	Tr	Tr	Tr	Tr	Tr	Tr	Tr
SiO_2	53.7	57.1	56.5	58.2	57.3	56.7	55.8	57.3	56.9	57.0	56.4	56.1	56.6	56.6	57.4	56.8	56.9	57.3	57.1	57.2	56.6	55.9
TiO_2	0.07	b.d.l.	b.d.l.	0.03	0.04	b.d.l.	0.01	0.02	b.d.l.	b.d.l.	b.d.l.	b.d.l.	0.03	b.d.l.	0.02	b.d.l.	0.01	b.d.l.	0.02	b.d.l.	b.d.l.	0.01
Al_2O_3	5.41	0.05	0.15	0.18	1.41	1.62	1.55	1.67	2.01	1.90	2.13	2.48	1.89	1.59	1.90	1.81	2.09	1.74	1.64	1.19	2.36	2.52
Cr_2O_3	0.46	b.d.l.	0.02	0.03	0.21	0.11	0.29	0.66	1.06	0.59	1.16	1.41	0.63	0.80	0.57	0.97	1.01	0.96	0.96	0.69	0.67	0.66
FeO	2.37	1.93	2.18	1.86	1.71	2.10	2.83	1.72	1.71	1.85	1.88	1.85	1.98	1.67	1.80	1.85	1.85	1.79	1.77	1.75	1.68	1.80
MnO	0.02	0.05	0.06	0.03	0.02	0.07	0.07	0.03	0.02	0.06	0.04	0.03	0.06	b.d.l.	0.04	0.06	b.d.l.	0.01	0.01	0.02	0.03	0.01
MgO	21.5	25.2	26.0	25.5	23.1	23.5	23.6	23.5	22.9	23.3	23.1	22.8	22.8	22.7	23.2	22.9	23.3	23.2	22.9	23.3	23.0	22.6
CaO	13.0	11.9	11.2	10.6	13.4	12.6	12.4	13.1	13.0	13.0	12.8	12.9	12.8	13.1	13.0	13.0	13.0	13.2	13.0	13.1	13.0	12.8
Na_2O	0.39	0.09	0.11	0.14	0.06	0.61	0.51	0.04	0.03	0.02	0.02	0.04	0.04	0.01	0.03	0.01	0.04	0.02	b.d.l.	0.01	0.08	0.11
K_2O	b.d.l.	0.02	0.01	0.04	0.01	b.d.l.	0.01	b.d.l.	0.01	b.d.l.	0.01	b.d.l.	0.01	b.d.l.	0.01	0.01	0.01	b.d.l.	b.d.l.	b.d.l.	0.01	b.d.l.
NiO	0.04	b.d.l.	0.02	0.03	0.05	0.06	0.04	0.08	0.07	0.08	0.04	0.11	0.08	0.05	0.10	0.06	0.14	0.04	0.03	0.09	0.09	0.06
Total	96.9	96.3	96.3	96.7	97.4	97.3	97.0	98.1	97.7	97.8	97.5	97.8	96.9	96.5	98.1	97.5	98.3	98.2	97.5	97.3	97.5	96.5
T(IV):																						
Si	7.417	7.992	7.976	7.968	7.845	7.753	7.746	7.780	7.770	7.764	7.720	7.675	7.794	7.835	7.810	7.781	7.724	7.784	7.832	7.841	7.734	7.724
Al	0.583	0.008	0.024	0.029	0.155	0.248	0.254	0.220	0.230	0.236	0.280	0.325	0.206	0.165	0.190	0.219	0.277	0.216	0.168	0.159	0.266	0.276
Ti	0.000	0.000	0.000	0.003	0.000	0.000	0.001	0.000	0.000	0.000	0.000	0.000	0.000	0.000	0.000	0.000	0.000	0.000	0.000	0.000	0.000	0.000
C(VI):																						
Al	0.297	0.000	0.000	0.000	0.072	0.014	0.000	0.047	0.094	0.068	0.064	0.075	0.100	0.094	0.115	0.073	0.057	0.062	0.097	0.033	0.115	0.133
Ti	0.007	0.000	0.000	0.000	0.004	0.000	0.000	0.002	0.000	0.000	0.000	0.000	0.003	0.000	0.002	0.000	0.001	0.000	0.002	0.000	0.000	0.001
Cr	0.050	0.000	0.003	0.004	0.023	0.012	0.031	0.071	0.115	0.064	0.125	0.152	0.068	0.087	0.062	0.105	0.109	0.104	0.104	0.075	0.072	0.073
Ni+Zn	0.004	0.000	0.002	0.004	0.005	0.006	0.004	0.009	0.007	0.009	0.004	0.012	0.008	0.006	0.011	0.006	0.016	0.004	0.003	0.010	0.010	0.006
Fe^{3+}	0.172	0.000	0.000	0.000	0.071	0.232	0.000	0.110	0.033	0.110	0.097	0.078	0.043	0.000	0.018	0.046	0.098	0.057	0.000	0.055	0.103	0.098
Mg	4.422	5.259	5.475	5.217	4.716	4.785	4.886	4.751	4.673	4.737	4.708	4.654	4.681	4.682	4.704	4.684	4.712	4.705	4.684	4.755	4.686	4.661
Fe^{2+}	0.101	0.226	0.257	0.214	0.125	0.008	0.328	0.085	0.162	0.101	0.117	0.134	0.185	0.194	0.187	0.166	0.112	0.146	0.203	0.146	0.089	0.111
Mn	0.002	0.006	0.007	0.003	0.002	0.008	0.008	0.003	0.003	0.007	0.004	0.004	0.007	0.000	0.005	0.007	0.000	0.001	0.001	0.003	0.003	0.001
B:																						
Ca	1.919	1.509	1.256	1.559	1.964	1.848	1.742	1.912	1.901	1.899	1.874	1.892	1.893	1.936	1.889	1.908	1.894	1.916	1.908	1.922	1.898	1.887
Na	0.026	0.000	0.000	0.000	0.017	0.087	0.000	0.011	0.009	0.006	0.006	0.000	0.009	0.001	0.007	0.003	0.001	0.006	0.000	0.003	0.022	0.029
A:																						
Ca	0.000	0.281	0.440	0.002	0.000	0.000	0.102	0.000	0.000	0.000	0.000	0.005	0.000	0.000	0.000	0.000	0.000	0.000	0.000	0.000	0.000	0.000
Na	0.077	0.026	0.030	0.037	0.000	0.075	0.138	0.000	0.000	0.000	0.000	0.010	0.000	0.000	0.000	0.000	0.009	0.000	0.000	0.000	0.000	0.000
K	0.000	0.004	0.003	0.007	0.001	0.000	0.002	0.000	0.002	0.000	0.001	0.000	0.002	0.000	0.001	0.002	0.001	0.000	0.000	0.000	0.002	0.000
Mg#	94.2	95.9	95.5	96.1	96.0	95.2	93.7	96.1	96.0	95.7	95.6	95.6	95.4	96.0	95.8	95.7	95.7	95.9	95.9	96.0	96.1	95.7
T (°C)	789	707	708	713	728	752	744	736	737	736	742	749	732	728	731	734	742	734	727	727	743	744
H_2O	3.07	3.68	3.69	3.33	2.63	2.67	2.96	1.88	2.30	2.22	2.51	2.19	3.13	3.48	1.92	2.53	1.70	1.76	2.54	2.66	2.48	3.48

This is the peer-reviewed, final accepted version for American Mineralogist, published by the Mineralogical Society of America.
The published version is subject to change. Cite as Authors (Year) Title. American Mineralogist, in press.
DOI: https://doi.org/10.2138/am-2021-7593. http://www.minsocam.org/

(Table 3 continued)

Sample	LN15-03																					
Rock	Harzburgite																					
Mineral	Amp[1]	Amp[1]	Amp[1]	Amp[1]	Amp[1]	Amp[1]	Amp[1]	Amp[1]	Amp[1]	Amp[1]	Amp[3]	Amp[3]	Amp[3]	Amp[3]	Amp[3]	Amp[3]	Amp[3]	Amp[3]	Amp[3]	Amp[3]	Amp[3]	Amp[3]
Type	Tr	Tr	Tr	Tr	Tr	Tr	Tr	Tr	Tr	Tr	Mhb	Mhb	Mhb	Mhb	Mhb	Mhb	Mhb	Mhb	Mhb	Mhb	Mhb	Mhb
SiO_2	57.1	57.3	57.3	56.8	55.8	55.7	54.7	57.9	57.7	56.4	53.8	53.8	52.9	52.7	52.9	52.7	52.5	52.7	52.2	52.5	50.6	51.0
TiO_2	0.01	b.d.l.	b.d.l.	b.d.l.	0.01	b.d.l.	0.04	b.d.l.	b.d.l.	b.d.l.	0.05	b.d.l.	b.d.l.	0.02	b.d.l.	0.05	0.03	0.06	0.06	0.06	b.d.l.	0.01
Al_2O_3	1.03	1.46	1.38	1.86	2.20	3.33	3.83	0.81	0.77	1.67	4.19	4.24	4.59	4.82	5.25	5.82	5.29	5.65	5.48	5.51	5.15	6.33
Cr_2O_3	0.19	0.39	0.38	0.41	0.75	0.96	1.02	0.31	0.21	0.37	1.83	1.83	1.90	2.43	2.51	1.96	2.11	2.11	2.20	1.89	4.29	2.37
FeO	1.72	1.88	1.80	1.92	1.98	1.94	2.07	1.65	1.80	1.78	2.09	2.16	2.15	2.28	2.17	2.16	2.30	2.22	2.21	2.66	2.51	2.20
MnO	0.01	b.d.l.	0.01	0.02	b.d.l.	0.02	0.01	0.01	0.05	0.02	0.02	0.04	0.02	b.d.l.	0.03	0.04	0.02	0.02	0.01	0.03	0.03	0.05
MgO	23.0	23.1	23.2	23.4	22.6	22.5	21.9	23.6	23.4	22.8	22.0	22.2	22.0	21.7	21.8	21.7	21.7	21.6	21.2	23.2	21.3	21.5
CaO	12.8	12.7	13.0	12.7	12.7	12.8	12.8	13.1	13.3	13.0	12.6	12.7	12.6	12.2	12.1	12.0	12.2	12.3	12.5	10.7	11.6	11.2
Na_2O	0.36	0.10	0.14	0.06	0.06	0.50	0.14	0.03	b.d.l.	0.04	0.39	0.38	0.48	0.59	0.95	0.68	0.80	0.74	0.59	0.73	0.63	1.14
K_2O	0.02	0.01	0.01	0.01	b.d.l.	0.03	b.d.l.	0.01	0.01	b.d.l.	0.11	0.12	0.14	0.11	0.02	0.03	0.07	0.06	0.18	0.07	0.04	0.05
NiO	0.04	0.06	0.04	0.06	0.05	0.08	0.05	0.07	0.08	0.08	0.11	0.08	0.05	0.10	0.03	0.05	0.12	0.05	0.05	0.02	0.09	0.05
Total	96.3	97.0	97.2	97.3	96.2	97.8	96.5	97.5	97.2	96.2	97.1	97.6	96.9	97.0	97.6	97.2	97.2	97.5	96.6	97.3	96.3	95.9
T(IV):																						
Si	7.884	7.871	7.844	7.768	7.738	7.615	7.569	7.910	7.903	7.816	7.456	7.425	7.363	7.344	7.314	7.302	7.301	7.296	7.294	7.264	7.179	7.170
Al	0.117	0.129	0.157	0.233	0.262	0.386	0.431	0.091	0.097	0.184	0.544	0.575	0.637	0.656	0.686	0.698	0.700	0.704	0.706	0.736	0.821	0.830
Ti	0.000	0.000	0.000	0.000	0.000	0.000	0.000	0.000	0.000	0.000	0.000	0.000	0.000	0.000	0.000	0.000	0.000	0.000	0.000	0.000	0.000	0.000
C(VI):																						
Al	0.050	0.107	0.066	0.067	0.098	0.151	0.194	0.040	0.027	0.088	0.140	0.116	0.115	0.135	0.171	0.252	0.167	0.218	0.197	0.164	0.040	0.220
Ti	0.001	0.000	0.000	0.000	0.001	0.000	0.005	0.000	0.000	0.000	0.005	0.000	0.000	0.003	0.000	0.005	0.003	0.006	0.006	0.006	0.000	0.001
Cr	0.021	0.042	0.041	0.045	0.082	0.104	0.111	0.033	0.023	0.040	0.200	0.199	0.209	0.268	0.275	0.215	0.232	0.231	0.243	0.207	0.481	0.263
Ni+Zn	0.005	0.007	0.004	0.007	0.006	0.008	0.006	0.008	0.009	0.009	0.012	0.009	0.005	0.012	0.004	0.005	0.013	0.005	0.006	0.002	0.010	0.005
Fe^{3+}	0.143	0.008	0.088	0.140	0.097	0.130	0.145	0.028	0.050	0.068	0.070	0.068	0.096	0.041	0.023	0.042	0.059	0.037	0.076	0.036	0.000	0.095
Mg	4.735	4.732	4.739	4.774	4.679	4.576	4.514	4.801	4.775	4.711	4.533	4.573	4.568	4.511	4.490	4.479	4.505	4.455	4.411	4.788	4.501	4.517
Fe^{2+}	0.055	0.209	0.118	0.080	0.133	0.092	0.095	0.160	0.157	0.139	0.173	0.181	0.154	0.224	0.227	0.209	0.208	0.221	0.182	0.273	0.298	0.164
Mn	0.001	0.000	0.001	0.003	0.000	0.002	0.002	0.002	0.006	0.002	0.002	0.005	0.002	0.000	0.004	0.005	0.003	0.002	0.002	0.003	0.003	0.006
B:																						
Ca	1.890	1.869	1.904	1.868	1.888	1.869	1.896	1.917	1.950	1.932	1.866	1.850	1.851	1.807	1.787	1.784	1.810	1.824	1.871	1.521	1.668	1.693
Na	0.096	0.027	0.037	0.016	0.017	0.068	0.033	0.008	0.001	0.011	0.000	0.000	0.000	0.000	0.020	0.004	0.000	0.001	0.007	0.000	0.000	0.035
A:																						
Ca	0.000	0.000	0.000	0.000	0.000	0.000	0.000	0.000	0.000	0.000	0.000	0.034	0.032	0.014	0.000	0.000	0.003	0.000	0.000	0.062	0.097	0.000
Na	0.000	0.000	0.000	0.000	0.000	0.063	0.004	0.000	0.000	0.000	0.104	0.102	0.129	0.160	0.234	0.179	0.216	0.197	0.153	0.196	0.174	0.275
K	0.003	0.001	0.001	0.002	0.000	0.006	0.000	0.002	0.002	0.000	0.020	0.022	0.025	0.020	0.003	0.005	0.012	0.010	0.032	0.012	0.007	0.009
Mg#	96.0	95.6	95.8	95.6	95.3	95.4	95.0	96.2	95.9	95.8	94.9	94.8	94.8	94.4	94.7	94.7	94.4	94.5	94.5	94.0	93.8	94.6
T (°C)	731	724	729	736	740	768	764	719	718	730	786	789	799	804	819	813	816	816	812	816	825	843
H_2O	3.70	3.03	2.76	2.69	3.75	2.23	3.51	2.49	2.76	3.84	2.87	2.44	3.07	3.02	2.37	2.84	2.81	2.51	3.43	2.71	3.75	4.07

Always consult and cite the final, published document. See http:/www.minsocam.org or GeoscienceWorld

This is the peer-reviewed, final accepted version for American Mineralogist, published by the Mineralogical Society of America.
The published version is subject to change. Cite as Authors (Year) Title. American Mineralogist, in press.
DOI: https://doi.org/10.2138/am-2021-7593. http://www.minsocam.org/

(Table 3 continued)

Sample																						
Rock																						
Mineral	Amp[3]	Amp[3]	Amp[3]	Amp[3]	Amp[3]	Amp[3]	Amp[3]	Amp[3]	Amp[3]	Amp[3]	Amp[3]	Amp[3]	Amp[3]	Amp[3]	Amp[3]	Amp[3]	Amp[3]	Amp[3]	Amp[3]	Amp[3]	Amp[3]	Amp[3]
Type	Mhb	Mhb	Mhb	Mhb	Mhb	Mhb	Mhb	Mhb	Mhb	Mhb	Mhb	Mhb	Mhb	Tr	Tr	Tr	Tr	Tr	Tr	Tr	Tr	Tr
SiO_2	51.0	50.9	50.9	51.1	51.1	49.8	48.9	49.6	49.6	48.2	54.4	53.6	51.9	56.2	55.5	55.5	55.5	55.7	55.6	55.3	55.1	55.6
TiO_2	0.03	0.01	0.05	0.06	0.05	0.12	0.06	0.05	0.06	0.08	0.04	0.05	0.04	b.d.l.	0.03	b.d.l.	b.d.l.	b.d.l.	0.03	b.d.l.	0.05	b.d.l.
Al_2O_3	6.23	6.30	6.28	6.52	6.71	7.81	7.77	7.24	7.85	8.37	4.43	4.46	5.96	1.43	2.38	2.48	2.35	2.49	2.75	2.67	2.64	2.56
Cr_2O_3	2.38	2.51	2.57	2.57	2.34	2.46	3.48	2.75	2.47	3.12	2.17	1.64	2.45	1.37	1.25	1.41	1.40	1.63	1.59	1.56	1.39	1.64
FeO	2.29	2.64	2.53	2.39	2.69	2.62	2.81	2.64	2.70	2.62	3.32	2.16	2.54	1.80	1.91	1.78	1.86	1.97	1.98	1.88	1.90	1.99
MnO	0.05	0.05	0.07	0.06	0.05	0.06	0.05	0.03	0.04	0.09	0.12	0.09	0.07	0.05	0.03	0.03	0.03	0.07	0.04	0.01	0.01	0.03
MgO	21.2	21.1	21.1	21.3	21.1	20.2	19.1	20.7	20.5	19.9	24.2	21.7	21.4	22.7	22.6	22.5	22.6	22.7	22.5	22.7	22.6	24.4
CaO	12.0	12.0	12.0	12.0	12.1	12.0	11.3	11.8	12.1	11.5	8.5	12.2	12.0	12.4	12.6	12.8	13.0	12.5	12.4	12.5	12.6	10.9
Na_2O	1.03	1.13	1.17	1.09	1.01	1.14	1.20	1.31	1.21	1.38	0.95	0.75	1.21	0.05	0.14	0.15	0.16	0.27	0.30	0.15	0.23	0.23
K_2O	0.02	0.04	0.05	0.04	0.04	0.03	0.04	0.04	0.03	0.06	0.04	0.11	0.10	0.04	0.07	0.08	0.07	0.04	0.03	0.06	0.08	0.03
NiO	0.09	0.12	0.06	0.06	0.04	0.08	0.08	0.10	0.09	0.10	0.04	0.07	0.07	0.07	0.10	0.11	0.07	0.04	0.03	0.11	0.12	0.02
Total	96.3	96.8	96.9	97.2	97.2	96.4	94.8	96.3	96.6	95.4	98.1	96.8	97.6	96.1	96.7	96.8	97.0	97.5	97.2	97.0	96.8	97.4
T(IV):																						
Si	7.168	7.142	7.137	7.133	7.130	7.021	7.011	7.011	6.988	6.885	7.450	7.442	7.206	7.820	7.677	7.668	7.661	7.657	7.647	7.634	7.627	7.620
Al	0.832	0.858	0.863	0.867	0.870	0.979	0.989	0.989	1.012	1.115	0.550	0.558	0.794	0.180	0.324	0.332	0.339	0.343	0.353	0.367	0.373	0.380
Ti	0.000	0.000	0.000	0.000	0.000	0.000	0.000	0.000	0.000	0.000	0.000	0.000	0.000	0.000	0.000	0.000	0.000	0.000	0.000	0.000	0.000	0.000
C(VI):																						
Al	0.199	0.184	0.175	0.206	0.234	0.317	0.324	0.217	0.290	0.296	0.165	0.173	0.182	0.055	0.065	0.072	0.043	0.061	0.093	0.068	0.058	0.034
Ti	0.003	0.001	0.005	0.007	0.005	0.012	0.006	0.005	0.006	0.009	0.004	0.005	0.004	0.000	0.003	0.000	0.000	0.000	0.003	0.000	0.005	0.000
Cr	0.264	0.278	0.285	0.284	0.259	0.274	0.395	0.307	0.275	0.353	0.234	0.180	0.270	0.150	0.137	0.154	0.153	0.177	0.173	0.170	0.152	0.178
Ni+Zn	0.010	0.013	0.007	0.007	0.005	0.009	0.009	0.011	0.010	0.012	0.005	0.008	0.007	0.007	0.012	0.012	0.008	0.005	0.003	0.012	0.014	0.002
Fe^{3+}	0.087	0.064	0.059	0.029	0.046	0.060	0.118	0.075	0.065	0.115	0.000	0.105	0.039	0.000	0.131	0.118	0.123	0.080	0.084	0.091	0.121	0.033
Mg	4.440	4.419	4.419	4.426	4.382	4.248	4.093	4.364	4.292	4.239	4.935	4.496	4.426	4.711	4.656	4.623	4.648	4.652	4.621	4.674	4.652	4.984
Fe^{2+}	0.182	0.245	0.238	0.250	0.268	0.249	0.220	0.237	0.253	0.198	0.380	0.145	0.256	0.210	0.089	0.088	0.092	0.147	0.144	0.126	0.099	0.196
Mn	0.006	0.006	0.008	0.007	0.006	0.007	0.006	0.003	0.004	0.011	0.014	0.010	0.009	0.006	0.004	0.004	0.003	0.008	0.005	0.001	0.002	0.004
B:																						
Ca	1.806	1.790	1.805	1.786	1.795	1.818	1.742	1.780	1.804	1.759	1.243	1.811	1.783	1.843	1.871	1.897	1.914	1.843	1.830	1.852	1.875	1.570
Na	0.004	0.000	0.000	0.000	0.000	0.006	0.087	0.000	0.000	0.009	0.020	0.067	0.024	0.013	0.033	0.032	0.017	0.027	0.044	0.006	0.022	0.000
A:																						
Ca	0.000	0.008	0.003	0.017	0.021	0.000	0.000	0.007	0.017	0.000	0.000	0.000	0.000	0.000	0.000	0.000	0.000	0.000	0.000	0.000	0.000	0.035
Na	0.278	0.308	0.319	0.296	0.272	0.306	0.247	0.358	0.330	0.373	0.232	0.137	0.303	0.000	0.006	0.007	0.026	0.045	0.036	0.034	0.039	0.061
K	0.003	0.007	0.009	0.006	0.006	0.005	0.006	0.008	0.005	0.012	0.007	0.019	0.017	0.006	0.012	0.014	0.011	0.007	0.006	0.010	0.015	0.006
Mg#	94.3	93.5	93.7	94.1	93.3	93.2	92.4	93.3	93.1	93.1	92.9	94.7	93.8	95.7	95.5	95.7	95.6	95.3	95.3	95.6	95.5	95.6
T (°C)	840	843	846	846	841	861	862	866	866	885	792	797	838	730	751	753	753	756	759	757	760	760
H_2O	3.67	3.16	3.11	2.80	2.77	3.60	5.19	3.73	3.40	4.64	1.86	3.21	2.37	3.92	3.32	3.16	2.96	2.54	2.77	2.95	3.23	2.61

(Table 3 continued)

Sample						LN15-07																
Rock						Harzburgite																
Mineral	Amp[3]	Amp[3]	Amp[3]	Amp[3]	Amp[3]	Amp[1]	Amp[1]	Amp[1]	Amp[1]	Amp[1]	Amp[1]	Amp[1]	Amp[1]	Amp[1]	Amp[1]	Amp[1]	Amp[1]	Amp[3]	Amp[3]	Amp[3]	Amp[3]	Amp[3]
Type	Tr	Tr	Tr	Tr	Tr	Tr	Tr	Tr	Tr	Tr	Tr	Tr	Tr	Tr	Tr	Tr	Tr	Tr	Tr	Tr	Tr	Tr
SiO_2	55.4	54.7	55.2	54.1	55.8	58.5	58.2	56.9	57.9	58.2	57.5	58.0	57.5	57.8	57.5	56.9	56.6	54.3	56.2	55.9	54.4	53.2
TiO_2	b.d.l.	0.01	0.02	0.03	0.10	0.02	0.01	b.d.l.	b.d.l.	0.01	0.04	0.02	0.05	0.01	0.01	0.01	0.01	b.d.l.	0.02	b.d.l.	0.04	b.d.l.
Al_2O_3	2.84	2.89	2.90	2.91	2.87	0.08	0.10	0.13	0.92	0.91	0.83	0.96	1.03	0.31	0.44	0.83	1.26	1.14	2.80	3.01	4.64	4.60
Cr_2O_3	1.73	1.63	1.75	1.94	1.60	0.02	0.04	b.d.l.	0.17	0.12	0.15	0.21	0.10	0.29	0.03	0.11	0.27	0.51	0.61	0.84	1.15	0.62
FeO	1.88	1.96	1.90	2.01	2.07	1.58	1.65	1.99	1.61	1.62	1.66	1.68	1.82	1.60	1.66	1.65	1.82	1.90	2.20	2.08	2.37	3.44
MnO	0.04	0.03	0.03	0.03	0.07	0.05	0.07	0.03	0.01	0.06	0.03	0.05	0.07	0.03	0.05	0.03	0.05	0.05	0.08	0.03	0.02	0.06
MgO	22.7	22.7	23.1	22.2	22.6	24.3	24.0	25.3	23.8	23.0	22.7	22.8	22.8	23.9	23.3	23.1	23.2	25.3	22.9	22.8	22.0	22.4
CaO	12.4	12.3	12.4	12.4	12.4	13.2	13.1	11.9	13.1	13.2	13.0	13.1	12.8	12.9	13.4	13.5	13.3	10.0	13.0	13.1	12.8	12.1
Na_2O	0.28	0.31	0.29	0.23	0.22	0.20	0.23	0.19	0.08	0.11	0.11	0.07	0.08	0.38	0.01	0.09	0.13	0.53	0.20	0.13	0.32	0.32
K_2O	b.d.l.	0.03	0.03	0.05	0.13	b.d.l.	b.d.l.	0.01	0.02	b.d.l.	b.d.l.	b.d.l.	b.d.l.	0.04	0.01	b.d.l.	b.d.l.	0.04	0.01	0.01	b.d.l.	0.03
NiO	0.06	0.07	0.09	0.05	0.11	0.09	0.09	0.14	0.02	0.07	0.10	0.07	0.08	0.06	0.08	0.09	0.05	0.05	0.08	0.07	0.12	0.12
Total	97.4	96.6	97.7	96.0	97.9	98.0	97.6	96.5	97.6	97.3	96.1	97.0	96.3	97.3	96.5	96.2	96.7	93.9	98.0	98.0	97.8	96.9
T(IV):																						
Si	7.618	7.583	7.580	7.557	7.638	7.985	7.982	7.979	7.889	7.984	7.982	7.980	7.962	7.948	7.943	7.880	7.795	7.807	7.656	7.624	7.466	7.386
Al	0.382	0.417	0.420	0.443	0.362	0.013	0.017	0.021	0.112	0.016	0.019	0.020	0.038	0.050	0.057	0.120	0.204	0.193	0.344	0.376	0.534	0.614
Ti	0.000	0.000	0.000	0.000	0.000	0.002	0.001	0.000	0.000	0.000	0.000	0.000	0.000	0.001	0.000	0.000	0.001	0.000	0.000	0.000	0.000	0.000
C(VI):																						
Al	0.078	0.055	0.048	0.036	0.101	0.000	0.000	0.000	0.035	0.131	0.117	0.135	0.130	0.000	0.015	0.015	0.000	0.000	0.105	0.107	0.217	0.139
Ti	0.000	0.001	0.002	0.003	0.010	0.000	0.000	0.000	0.000	0.001	0.004	0.002	0.005	0.000	0.001	0.001	0.000	0.000	0.002	0.000	0.004	0.000
Cr	0.188	0.179	0.190	0.214	0.173	0.002	0.005	0.000	0.018	0.013	0.017	0.023	0.011	0.031	0.003	0.012	0.029	0.058	0.065	0.090	0.125	0.068
Ni+Zn	0.006	0.007	0.010	0.006	0.012	0.010	0.010	0.016	0.002	0.008	0.011	0.007	0.009	0.006	0.009	0.010	0.005	0.006	0.009	0.007	0.013	0.014
Fe^{3+}	0.068	0.112	0.055	0.130	0.044	0.000	0.000	0.000	0.081	0.000	0.000	0.000	0.000	0.000	0.040	0.062	0.209	0.000	0.144	0.129	0.092	0.178
Mg	4.665	4.688	4.723	4.631	4.605	4.935	4.911	5.287	4.825	4.693	4.692	4.676	4.705	4.893	4.791	4.767	4.756	5.422	4.645	4.645	4.492	4.648
Fe^{2+}	0.148	0.116	0.162	0.104	0.193	0.180	0.189	0.233	0.102	0.186	0.193	0.194	0.211	0.184	0.152	0.129	0.000	0.229	0.107	0.109	0.180	0.221
Mn	0.005	0.004	0.004	0.003	0.008	0.006	0.008	0.003	0.001	0.007	0.004	0.006	0.008	0.003	0.005	0.004	0.005	0.006	0.009	0.003	0.002	0.007
B:																						
Ca	1.828	1.828	1.805	1.863	1.826	1.867	1.878	1.460	1.912	1.932	1.933	1.937	1.900	1.883	1.980	2.000	1.959	1.279	1.901	1.909	1.876	1.726
Na	0.014	0.010	0.000	0.008	0.028	0.000	0.000	0.000	0.020	0.029	0.029	0.020	0.021	0.000	0.002	0.000	0.036	0.000	0.013	0.000	0.000	0.000
A:																						
Ca	0.000	0.000	0.020	0.000	0.000	0.057	0.047	0.328	0.000	0.000	0.000	0.000	0.000	0.017	0.000	0.002	0.000	0.266	0.000	0.007	0.004	0.070
Na	0.061	0.073	0.077	0.054	0.030	0.052	0.060	0.051	0.000	0.000	0.000	0.000	0.000	0.101	0.000	0.025	0.000	0.147	0.039	0.034	0.085	0.085
K	0.001	0.004	0.005	0.009	0.023	0.000	0.000	0.002	0.003	0.000	0.000	0.000	0.000	0.006	0.002	0.000	0.000	0.008	0.001	0.002	0.000	0.005
Mg#	95.6	95.4	95.6	95.2	95.1	96.5	96.3	95.8	96.3	96.2	96.0	96.0	95.7	96.4	96.2	96.1	95.8	96.0	94.9	95.1	94.3	92.1
T (°C)	762	767	768	768	758	714	715	711	723	711	712	711	712	724	714	724	736	744	753	756	780	782
H_2O	2.64	3.39	2.25	4.03	2.09	2.01	2.42	3.49	2.42	2.74	3.92	3.06	3.70	2.70	3.54	3.79	3.31	6.15	1.99	2.00	2.22	3.15

This is the peer-reviewed, final accepted version for American Mineralogist, published by the Mineralogical Society of America.
The published version is subject to change. Cite as Authors (Year) Title. American Mineralogist, in press.
DOI: https://doi.org/10.2138/am-2021-7593. http://www.minsocam.org/

(Table 3 continued)

Sample												LN15-11		18LN07-5								
Rock												Harzburgite		Dunite								
Mineral	Amp[3]	Amp[3]	Amp[3]	Amp[3]	Amp[3]	Amp[3]	Amp[3]	Amp[3]	Amp[3]	Amp[3]	Amp[3]	Amp[1]	Amp[1]	Amp[1]	Amp[1]	Amp[1]	Amp[1]	Amp[1]	Amp[1]	Amp[1]	Amp[1]	Amp[1]
Type	Tr	Tr	Tr	Tr	Tr	Tr	Tr	Tr	Tr	Tr	Tr	Tr	Tr	Ed	Ed	Ed	Ed	Ed	Ed	Mhb	Mhb	Tr
SiO_2	52.4	51.2	50.2	50.2	49.7	48.9	54.8	56.1	55.8	54.2	50.4	58.7	54.5	45.2	47.3	46.8	46.3	46.5	45.7	48.9	47.1	55.1
TiO_2	0.03	0.10	0.08	0.07	0.11	0.09	0.05	0.02	0.04	0.11	0.13	b.d.l.	0.03	0.48	0.27	0.49	0.48	0.41	0.44	0.12	0.29	0.05
Al_2O_3	5.74	7.01	8.81	8.54	8.58	8.86	1.12	2.78	3.22	5.23	8.54	0.02	2.83	11.6	9.31	10.8	10.8	9.97	11.8	8.83	8.38	2.18
Cr_2O_3	1.86	1.99	2.04	2.38	2.14	1.98	0.63	0.44	0.94	1.54	1.91	b.d.l.	0.59	1.98	2.35	1.70	1.83	2.76	2.09	2.25	2.26	0.61
FeO	2.59	2.60	2.63	2.76	3.29	2.78	1.73	2.91	2.10	2.33	2.70	1.65	2.30	2.00	1.93	2.37	2.49	2.02	2.52	1.87	1.81	1.50
MnO	0.02	0.06	0.05	0.03	0.06	0.05	0.06	0.09	0.04	0.07	0.09	0.04	0.07	0.04	0.05	0.04	0.06	0.04	0.07	0.02	0.07	0.07
MgO	21.1	20.6	19.9	20.3	20.1	19.3	22.4	23.2	22.4	21.1	19.7	23.9	22.4	18.7	19.6	19.8	19.6	20.2	18.9	20.6	19.5	22.9
CaO	12.7	12.8	12.9	12.3	12.3	12.5	12.3	11.8	12.4	12.4	12.6	13.4	12.9	12.2	12.2	12.2	12.5	11.0	12.4	12.3	12.0	12.6
Na_2O	0.44	0.61	0.56	0.90	0.54	0.56	0.07	0.17	0.47	0.43	0.72	b.d.l.	0.21	2.37	2.03	2.02	1.98	2.07	2.26	1.73	2.07	0.66
K_2O	0.03	0.01	0.01	b.d.l.	0.02	0.03	b.d.l.	0.01	0.01	b.d.l.	0.03	b.d.l.	b.d.l.	0.36	0.21	0.25	0.28	0.20	0.28	0.08	0.19	0.03
NiO	0.06	0.07	0.08	0.04	0.04	0.08	b.d.l.	0.06	0.13	0.09	0.08	0.10	0.03	0.09	0.09	0.14	0.13	0.06	0.10	0.09	0.12	0.15
Total	97.0	97.1	97.2	97.5	96.7	95.1	93.0	97.5	97.6	97.5	96.8	97.8	95.8	95.1	95.3	96.7	96.4	95.2	96.5	96.7	93.7	95.9
T(IV):																						
Si	7.294	7.145	7.000	6.994	6.979	6.958	7.807	7.681	7.644	7.467	7.053	7.998	7.596	6.503	6.754	6.625	6.586	6.661	6.501	6.863	6.828	7.655
Al	0.706	0.855	1.000	1.006	1.021	1.042	0.188	0.319	0.356	0.533	0.947	0.002	0.404	1.497	1.246	1.376	1.414	1.339	1.500	1.137	1.172	0.345
Ti	0.000	0.000	0.000	0.000	0.000	0.000	0.006	0.000	0.000	0.000	0.000	0.000	0.000	0.000	0.000	0.000	0.000	0.000	0.000	0.000	0.000	0.000
C(VI):																						
Al	0.234	0.298	0.449	0.397	0.400	0.445	0.000	0.129	0.163	0.316	0.461	0.000	0.061	0.468	0.322	0.424	0.395	0.346	0.476	0.326	0.259	0.012
Ti	0.004	0.011	0.009	0.008	0.012	0.009	0.000	0.002	0.004	0.011	0.014	0.000	0.003	0.052	0.030	0.052	0.052	0.045	0.047	0.013	0.031	0.005
Cr	0.205	0.219	0.225	0.262	0.238	0.223	0.071	0.047	0.102	0.168	0.211	0.000	0.065	0.226	0.265	0.190	0.205	0.313	0.235	0.250	0.259	0.067
Ni+Zn	0.006	0.008	0.009	0.004	0.005	0.009	0.000	0.006	0.014	0.010	0.009	0.011	0.003	0.011	0.010	0.016	0.015	0.007	0.012	0.010	0.014	0.016
Fe^{3+}	0.076	0.051	0.018	0.008	0.066	0.157	0.206	0.137	0.112	0.038	0.041	0.000	0.255	0.230	0.171	0.137	0.155	0.190	0.140	0.084	0.220	0.174
Mg	4.379	4.290	4.138	4.213	4.201	4.096	4.751	4.728	4.580	4.327	4.099	4.853	4.646	4.013	4.181	4.174	4.149	4.311	4.012	4.317	4.208	4.745
Fe^{2+}	0.225	0.253	0.289	0.313	0.320	0.175	0.000	0.195	0.128	0.230	0.275	0.188	0.014	0.010	0.060	0.144	0.141	0.053	0.160	0.135	0.000	0.000
Mn	0.002	0.007	0.006	0.004	0.007	0.005	0.007	0.011	0.005	0.008	0.010	0.004	0.009	0.004	0.006	0.004	0.007	0.005	0.008	0.003	0.009	0.008
B:																						
Ca	1.868	1.865	1.858	1.790	1.752	1.882	1.873	1.723	1.815	1.831	1.879	1.944	1.923	1.886	1.868	1.855	1.882	1.690	1.887	1.845	1.856	1.884
Na	0.000	0.000	0.000	0.000	0.000	0.000	0.020	0.023	0.078	0.062	0.000	0.000	0.021	0.100	0.087	0.004	0.000	0.040	0.023	0.018	0.144	0.089
A:																						
Ca	0.030	0.051	0.069	0.045	0.095	0.026	0.000	0.000	0.000	0.000	0.003	0.011	0.000	0.000	0.000	0.000	0.016	0.000	0.000	0.000	0.000	0.000
Na	0.119	0.164	0.152	0.244	0.148	0.153	0.000	0.024	0.048	0.053	0.195	0.000	0.037	0.561	0.477	0.550	0.545	0.535	0.600	0.454	0.439	0.088
K	0.005	0.001	0.001	0.000	0.003	0.005	0.000	0.002	0.001	0.000	0.005	0.000	0.001	0.066	0.039	0.044	0.051	0.036	0.051	0.015	0.035	0.005
Mg#	93.6	93.4	93.1	92.9	91.6	92.5	95.9	93.4	95.0	94.2	92.8	96.3	94.5	94.3	94.8	93.7	93.4	94.7	93.0	95.2	95.0	96.5
T (°C)	804	829	847	856	844	851	733	743	763	784	844	706	760	974	929	945	948	944	966	904	922	771
H_2O	2.96	2.85	2.78	2.51	3.26	4.87	6.96	2.46	2.40	2.46	3.20	2.22	4.23	4.86	4.66	3.35	3.58	4.84	3.49	3.25	6.27	4.14

Always consult and cite the final, published document. See http:/www.minsocam.org or GeoscienceWorld

This is the peer-reviewed, final accepted version for American Mineralogist, published by the Mineralogical Society of America.
The published version is subject to change. Cite as Authors (Year) Title. American Mineralogist, in press.
DOI: https://doi.org/10.2138/am-2021-7593. http://www.minsocam.org/

(Table 3 continued)

Sample													LN15-06					18LN05-4				
Rock													Dunite					Chromitite				
Mineral	Amp[1]	Amp[1]	Amp[1]	Amp[1]	Amp[1]	Amp[1]	Amp[1]	Amp[1]	Amp[2]	Amp[2]	Amp[2]	Amp[2]	Amp[1]	Amp[1]	Amp[1]	Amp[1]	Amp[1]	Amp[1]	Amp[1]	Amp[1]	Amp[1]	Amp[1]
Type	Tr	Tr	Tr	Tr	Tr	Tr	Tr	Tr	Ed	Ed	Ed	Mhb	Tr	Tr	Tr	Tr	Tr	Tr	Tr	Tr	Tr	Tr
SiO_2	54.8	58.8	57.7	58.2	58.7	58.2	57.4	55.9	46.4	45.7	45.8	47.7	56.8	57.2	58.1	57.0	56.9	57.2	57.0	55.6	55.7	53.8
TiO_2	0.13	b.d.l.	b.d.l.	0.02	0.06	0.04	0.02	0.08	0.29	0.50	0.36	0.25	b.d.l.	0.03	0.04	b.d.l.	0.01	0.01	0.04	0.04	b.d.l.	b.d.l.
Al_2O_3	2.53	0.15	0.21	0.22	0.23	0.80	0.84	1.75	11.0	10.3	11.9	10.5	0.12	0.12	0.27	1.63	1.61	1.59	1.46	1.49	1.71	1.81
Cr_2O_3	0.78	0.02	0.29	0.20	0.06	0.04	0.24	0.17	1.89	1.94	1.96	1.84	1.14	0.21	0.21	0.42	0.33	0.66	0.76	0.57	0.47	0.51
FeO	1.49	0.67	0.37	0.64	0.80	0.83	0.75	0.60	2.07	1.93	2.00	1.92	1.87	1.07	0.65	0.78	1.19	0.68	0.65	0.66	0.68	0.67
MnO	0.03	0.01	b.d.l.	0.02	0.03	0.03	0.03	b.d.l.	0.03	0.03	0.04	0.06	0.01	0.04	b.d.l.	0.02	0.03	0.02	0.01	0.03	0.01	b.d.l.
MgO	22.9	24.6	23.7	24.1	24.8	24.3	24.0	22.8	19.9	19.1	19.2	20.0	24.4	24.3	24.5	23.3	23.5	24.2	24.2	23.4	23.5	24.2
CaO	12.6	13.0	13.4	13.2	12.9	13.3	13.2	13.3	12.2	12.2	12.3	12.3	10.8	13.0	13.6	13.1	13.4	12.5	12.6	12.3	12.5	11.9
Na_2O	0.70	0.12	0.14	0.09	0.12	0.19	0.18	0.36	1.76	2.29	1.92	1.70	0.59	0.55	0.18	0.28	0.36	0.59	0.58	0.59	0.59	0.58
K_2O	0.05	b.d.l.	b.d.l.	0.01	b.d.l.	0.01	0.01	0.02	0.10	0.29	0.18	0.12	0.02	0.02	b.d.l.	b.d.l.	b.d.l.	0.01	0.02	0.02	0.01	0.02
NiO	0.20	0.05	0.04	0.12	0.14	0.08	0.10	0.10	0.10	0.13	0.10	0.09	0.06	0.05	0.02	0.05	0.09	0.11	0.13	0.16	0.17	0.08
Total	96.2	97.5	95.9	96.7	97.8	97.8	96.8	95.1	95.8	94.3	95.8	96.5	95.8	96.6	97.5	96.7	97.5	97.6	97.5	94.9	95.3	93.5
T(IV):																						
Si	7.605	7.988	7.986	7.963	7.958	7.877	7.863	7.830	6.598	6.602	6.522	6.714	7.980	7.978	7.952	7.826	7.768	7.770	7.764	7.752	7.731	7.695
Al	0.395	0.012	0.014	0.035	0.037	0.123	0.136	0.170	1.402	1.398	1.478	1.286	0.020	0.019	0.044	0.174	0.232	0.230	0.235	0.244	0.269	0.305
Ti	0.000	0.000	0.000	0.002	0.006	0.000	0.001	0.000	0.000	0.000	0.000	0.000	0.000	0.003	0.004	0.000	0.000	0.000	0.001	0.004	0.000	0.000
C(VI):																						
Al	0.019	0.012	0.021	0.000	0.000	0.005	0.000	0.120	0.445	0.350	0.522	0.464	0.000	0.000	0.000	0.090	0.027	0.025	0.000	0.000	0.011	0.000
Ti	0.014	0.000	0.000	0.000	0.000	0.004	0.001	0.009	0.031	0.054	0.039	0.026	0.000	0.000	0.000	0.000	0.001	0.001	0.003	0.000	0.000	0.000
Cr	0.085	0.002	0.032	0.022	0.007	0.005	0.026	0.018	0.212	0.222	0.221	0.205	0.126	0.023	0.022	0.046	0.036	0.071	0.082	0.062	0.052	0.058
Ni+Zn	0.023	0.005	0.004	0.013	0.015	0.009	0.011	0.011	0.011	0.015	0.012	0.010	0.007	0.006	0.002	0.006	0.010	0.012	0.014	0.018	0.019	0.009
Fe^{3+}	0.173	0.029	0.000	0.067	0.000	0.094	0.086	0.000	0.184	0.234	0.180	0.099	0.000	0.000	0.000	0.090	0.135	0.078	0.074	0.076	0.079	0.000
Mg	4.736	4.978	4.900	4.912	5.014	4.897	4.888	4.771	4.229	4.122	4.087	4.200	5.120	5.062	4.987	4.767	4.787	4.909	4.904	4.867	4.868	5.159
Fe^{2+}	0.000	0.048	0.043	0.006	0.091	0.000	0.000	0.071	0.062	0.000	0.058	0.128	0.219	0.125	0.075	0.000	0.000	0.000	0.000	0.000	0.000	0.080
Mn	0.003	0.002	0.000	0.002	0.004	0.003	0.003	0.000	0.004	0.004	0.005	0.008	0.001	0.005	0.000	0.002	0.003	0.003	0.001	0.003	0.001	0.000
B:																						
Ca	1.876	1.894	1.990	1.938	1.869	1.931	1.935	1.999	1.823	1.890	1.877	1.861	1.526	1.780	1.914	1.929	1.964	1.818	1.846	1.834	1.856	1.695
Na	0.071	0.031	0.011	0.025	0.000	0.050	0.048	0.001	0.000	0.110	0.000	0.000	0.000	0.000	0.000	0.072	0.036	0.084	0.076	0.138	0.114	0.000
A:																						
Ca	0.000	0.000	0.000	0.000	0.000	0.000	0.000	0.000	0.038	0.000	0.003	0.001	0.099	0.164	0.073	0.000	0.000	0.000	0.000	0.000	0.000	0.133
Na	0.118	0.000	0.027	0.000	0.030	0.000	0.000	0.096	0.485	0.533	0.530	0.464	0.161	0.149	0.047	0.003	0.059	0.072	0.077	0.020	0.044	0.162
K	0.009	0.000	0.001	0.002	0.000	0.002	0.002	0.004	0.019	0.053	0.033	0.021	0.003	0.004	0.000	0.000	0.001	0.002	0.003	0.004	0.001	0.004
Mg#	96.5	98.5	99.1	98.5	98.2	98.1	98.3	98.5	94.5	94.6	94.5	94.9	95.9	97.6	98.5	98.1	97.3	98.4	98.5	98.5	98.4	98.5
T (°C)	780	718	722	722	722	734	736	748	941	960	957	924	723	729	725	743	750	760	761	763	765	770
H_2O	3.82	2.55	4.14	3.26	2.20	2.19	3.25	4.89	4.20	5.66	4.24	3.47	4.21	3.43	2.47	3.35	2.51	2.38	2.54	5.13	4.66	6.48

Always consult and cite the final, published document. See http:/www.minsocam.org or GeoscienceWorld

This is the peer-reviewed, final accepted version for American Mineralogist, published by the Mineralogical Society of America.
The published version is subject to change. Cite as Authors (Year) Title. American Mineralogist, in press.
DOI: https://doi.org/10.2138/am-2021-7593. http://www.minsocam.org/

(Table 3 continued)

Sample			18LN05-6							18LN05-7								18LN05-8				
Rock			Chromitite							Chromitite								Chromitite				
Mineral	Amp[1]	Amp[1]	Amp[1]	Amp[1]	Amp[1]	Amp[1]	Amp[3]	Amp[3]	Amp[3]	Amp[1]	Amp[1]	Amp[1]	Amp[1]	Amp[1]	Amp[1]	Amp[1]	Amp[1]	Amp[1]	Amp[1]	Amp[1]	Amp[3]	Amp[3]
Type	Tr	Tr	Mhb	Tr	Tr	Tr	Ed	Mhb	Mhb	Tr	Tr	Tr	Tr	Tr	Tr	Tr	Tr	Tr	Tr	Tr	Ed	Mhb
SiO_2	55.6	56.0	52.1	56.7	56.2	55.2	45.9	45.9	47.9	57.3	57.3	56.7	57.3	56.4	57.5	55.7	54.9	57.7	55.2	57.6	47.7	50.8
TiO_2	0.01	0.01	0.17	0.02	0.08	0.11	0.19	0.21	0.23	b.d.l.	b.d.l.	0.03	0.03	b.d.l.	b.d.l.	0.02	0.02	0.04	0.01	0.01	0.15	0.09
Al_2O_3	2.48	2.59	4.29	1.64	2.30	3.21	10.0	7.94	9.13	0.37	0.37	0.85	0.89	1.09	1.08	1.83	2.09	0.07	0.11	0.15	9.36	6.13
Cr_2O_3	0.45	0.64	1.24	0.80	0.28	0.93	2.67	2.75	2.41	0.13	0.14	0.05	0.26	0.21	0.10	0.44	0.77	0.09	0.06	0.06	2.52	1.73
FeO	0.69	1.09	1.42	0.69	1.32	0.91	2.11	2.07	1.90	0.53	0.44	0.55	0.63	0.59	0.66	1.05	1.07	0.23	0.28	0.32	2.15	1.78
MnO	0.01	b.d.l.	0.03	0.03	0.04	0.01	0.02	0.06	0.04	0.03	b.d.l.	0.01	0.01	0.05	0.05	0.01	b.d.l.	b.d.l.	0.01	b.d.l.	0.06	0.03
MgO	23.4	23.6	21.8	24.4	23.4	22.6	19.3	18.8	20.4	24.0	24.6	23.7	24.3	23.5	24.4	23.5	23.0	24.8	25.8	24.9	20.4	21.3
CaO	12.8	13.1	12.6	11.7	12.7	12.9	12.8	12.6	12.6	13.2	12.8	12.8	13.0	13.0	12.5	13.0	12.8	11.3	11.6	11.7	12.2	12.7
Na_2O	0.75	0.69	1.04	0.55	0.58	0.73	1.91	1.41	1.70	0.31	0.32	0.32	0.37	0.38	0.56	0.59	0.65	1.32	0.18	1.31	1.91	1.11
K_2O	0.02	0.02	0.07	0.07	0.07	0.05	0.05	0.04	0.04	b.d.l.	b.d.l.	0.02	0.03	0.04	b.d.l.	0.02	0.02	0.02	0.03	0.04	0.03	0.04
NiO	0.16	0.08	0.16	0.14	0.11	0.16	0.14	0.12	0.15	0.12	0.12	0.16	0.14	0.12	0.16	0.11	0.15	0.11	0.28	0.12	0.15	0.17
Total	96.3	97.9	94.9	96.7	97.1	96.7	95.2	91.9	96.5	96.0	96.1	95.2	96.9	95.4	97.1	96.3	95.4	95.6	93.6	96.2	96.6	95.8
T(IV):																						
Si	7.659	7.622	7.358	7.764	7.695	7.602	6.604	6.817	6.774	7.939	7.939	7.865	7.854	7.840	7.837	7.700	7.654	7.985	7.980	7.975	6.741	7.154
Al	0.341	0.378	0.642	0.236	0.305	0.398	1.396	1.183	1.226	0.061	0.061	0.135	0.144	0.160	0.163	0.297	0.343	0.011	0.019	0.024	1.259	0.846
Ti	0.000	0.000	0.000	0.000	0.000	0.000	0.000	0.000	0.000	0.000	0.000	0.000	0.003	0.000	0.000	0.002	0.003	0.004	0.001	0.001	0.000	0.000
C(VI):																						
Al	0.062	0.037	0.073	0.029	0.065	0.123	0.302	0.208	0.295	0.000	0.000	0.004	0.000	0.019	0.010	0.000	0.000	0.000	0.000	0.000	0.300	0.171
Ti	0.001	0.001	0.018	0.002	0.008	0.012	0.021	0.024	0.025	0.000	0.000	0.003	0.000	0.000	0.000	0.000	0.000	0.000	0.000	0.000	0.016	0.010
Cr	0.049	0.068	0.138	0.087	0.031	0.102	0.304	0.323	0.270	0.014	0.015	0.005	0.028	0.023	0.011	0.049	0.085	0.010	0.007	0.006	0.282	0.193
Ni+Zn	0.018	0.009	0.018	0.016	0.012	0.018	0.016	0.014	0.017	0.014	0.014	0.018	0.015	0.014	0.017	0.012	0.016	0.012	0.032	0.013	0.017	0.020
Fe^{3+}	0.080	0.124	0.168	0.079	0.151	0.104	0.204	0.169	0.087	0.000	0.000	0.064	0.067	0.069	0.075	0.121	0.125				0.085	0.176
Mg	4.804	4.799	4.587	4.984	4.783	4.640	4.141	4.167	4.289	4.956	5.083	4.911	4.956	4.869	4.956	4.837	4.777	5.122	5.561	5.141	4.305	4.471
Fe^{2+}	0.000	0.000	0.000	0.000	0.000	0.000	0.050	0.088	0.138	0.061	0.052	0.000	0.005	0.000	0.000	0.000	0.000	0.026	0.034	0.037	0.169	0.034
Mn	0.001	0.000	0.003	0.003	0.004	0.001	0.002	0.008	0.005	0.003	0.000	0.001	0.001	0.005	0.006	0.002	0.000	0.000	0.001	0.000	0.008	0.004
B:																						
Ca	1.887	1.916	1.907	1.711	1.862	1.900	1.959	2.000	1.875	1.953	1.837	1.905	1.901	1.942	1.822	1.928	1.917	1.671	1.365	1.728	1.819	1.911
Na	0.099	0.045	0.089	0.089	0.084	0.100	0.000	0.000	0.000	0.000	0.000	0.086	0.027	0.058	0.102	0.051	0.081	0.159	0.000	0.075	0.000	0.011
A:																						
Ca	0.000	0.000	0.000	0.000	0.000	0.000	0.016	0.012	0.031	0.009	0.070	0.000	0.000	0.000	0.000	0.000	0.000	0.000	0.429	0.000	0.022	0.000
Na	0.100	0.138	0.194	0.058	0.071	0.096	0.533	0.405	0.467	0.083	0.085	0.000	0.071	0.044	0.046	0.107	0.096	0.195	0.049	0.277	0.524	0.292
K	0.003	0.003	0.013	0.012	0.011	0.009	0.008	0.008	0.008	0.000	0.001	0.004	0.005	0.006	0.000	0.004	0.004	0.004	0.005	0.007	0.005	0.007
Mg#	98.4	97.5	96.5	98.4	96.9	97.8	94.2	94.2	95.0	98.8	99.0	98.7	98.6	98.6	98.5	97.6	97.5	99.5	99.4	99.3	94.4	95.5
T (°C)	779	779	824	760	766	786	943	902	916	731	732	742	744	746	751	767	775	756	724	756	924	849
H_2O	3.66	2.15	5.12	3.28	2.95	3.28	4.84	8.07	3.55	4.02	3.90	4.82	3.10	4.60	2.95	3.71	4.55	4.37	6.45	3.83	3.40	4.19

Always consult and cite the final, published document. See http:/www.minsocam.org or GeoscienceWorld

This is the peer-reviewed, final accepted version for American Mineralogist, published by the Mineralogical Society of America.
The published version is subject to change. Cite as Authors (Year) Title. American Mineralogist, in press.
DOI: https://doi.org/10.2138/am-2021-7593. http://www.minsocam.org/

(Table 3 continued)

Sample									18LN05-9			18LN07-3										
Rock									Chromitite			Chromitite										
Mineral	Amp[3]	Amp[3]	Amp[3]	Amp[3]	Amp[3]	Amp[3]	Amp[3]	Amp[3]	Amp[1]	Amp[1]	Amp[1]	Amp[1]	Amp[1]	Amp[1]	Amp[1]	Amp[1]	Amp[1]	Amp[1]	Amp[1]	Amp[1]	Amp[1]	Amp[1]
Type	Mhb	Mhb	Mhb	Mhb	Mhb	Mhb	Mhb	Mhb	Tr	Tr	Tr	Mhb	Mhb	Mhb	Tr	Tr	Tr	Tr	Tr	Tr	Tr	Tr
SiO_2	49.4	49.9	49.5	47.7	48.2	47.7	47.3	47.3	57.8	55.0	57.1	51.7	51.3	49.2	57.7	57.2	57.1	56.6	56.1	57.2	55.4	56.4
TiO_2	0.21	0.17	0.15	0.16	0.19	0.25	0.18	0.19	b.d.l.	0.09	0.06	0.06	0.10	0.11	0.01	b.d.l.	b.d.l.	0.01	b.d.l.	0.07	0.04	0.03
Al_2O_3	7.36	7.82	8.13	8.16	9.04	8.95	9.21	9.51	0.04	0.16	0.20	5.16	5.84	6.67	0.21	0.23	0.60	0.87	0.81	0.84	1.11	1.08
Cr_2O_3	2.04	2.05	2.28	2.33	2.66	2.53	2.48	2.58	0.10	0.15	0.07	1.55	1.80	2.20	0.10	0.04	0.25	0.23	0.19	0.24	0.34	0.31
FeO	1.63	1.71	1.87	2.09	1.96	1.80	1.89	1.74	0.14	0.24	0.21	1.24	1.25	1.29	0.49	0.49	0.48	0.56	0.47	0.53	0.57	0.58
MnO	0.03	0.06	0.07	0.01	0.05	0.01	0.03	0.01	b.d.l.	0.02	b.d.l.	0.02	b.d.l.	b.d.l.	b.d.l.	b.d.l.	0.01	0.04	b.d.l.	0.01	b.d.l.	0.01
MgO	20.6	20.9	20.8	20.0	20.8	20.3	20.0	19.8	23.9	26.2	25.0	21.9	21.7	20.9	23.9	23.9	23.8	23.5	23.5	24.2	23.2	23.8
CaO	12.7	12.5	12.5	12.1	12.2	12.8	12.8	12.9	12.3	9.9	11.1	12.5	12.7	12.6	13.4	13.1	13.2	12.8	13.1	13.0	12.8	13.0
Na_2O	1.25	1.55	1.66	1.77	1.80	1.59	1.60	1.72	1.09	1.32	1.19	1.18	1.35	1.54	0.17	0.18	0.24	0.32	0.32	0.29	0.33	0.34
K_2O	0.05	b.d.l.	0.03	0.10	0.02	0.03	0.05	0.03	0.01	0.03	0.03	0.16	0.14	0.22	0.01	0.02	b.d.l.	0.04	0.01	b.d.l.	0.04	0.02
NiO	0.13	0.15	0.12	0.14	0.17	0.10	0.13	0.12	0.11	0.36	0.38	0.11	0.06	0.10	0.08	0.11	0.11	0.12	0.11	0.15	0.09	0.11
Total	95.4	96.7	97.1	94.6	97.1	96.2	95.8	95.9	95.5	93.4	95.4	95.6	96.2	94.9	96.1	95.3	95.8	95.1	94.7	96.5	93.9	95.6
T(IV):																						
Si	7.006	6.987	6.935	6.852	6.774	6.768	6.742	6.720	8.000	7.964	7.960	7.267	7.185	7.019	7.972	7.963	7.902	7.867	7.866	7.856	7.823	7.821
Al	0.994	1.013	1.065	1.148	1.226	1.232	1.258	1.280	0.000	0.027	0.033	0.733	0.815	0.981	0.028	0.037	0.098	0.133	0.134	0.137	0.177	0.176
Ti	0.000	0.000	0.000	0.000	0.000	0.000	0.000	0.000	0.000	0.009	0.006	0.000	0.000	0.000	0.000	0.000	0.000	0.000	0.000	0.007	0.000	0.003
C(VI):																						
Al	0.237	0.279	0.276	0.234	0.273	0.263	0.289	0.314	0.006	0.000	0.000	0.121	0.149	0.140	0.005	0.000	0.000	0.010	0.000	0.000	0.007	0.000
Ti	0.022	0.018	0.016	0.017	0.020	0.027	0.019	0.021	0.000	0.000	0.000	0.006	0.010	0.012	0.001	0.000	0.000	0.001	0.000	0.000	0.004	0.000
Cr	0.229	0.228	0.252	0.265	0.295	0.284	0.279	0.290	0.010	0.017	0.008	0.172	0.199	0.248	0.011	0.004	0.027	0.026	0.021	0.026	0.038	0.034
Ni+Zn	0.015	0.017	0.013	0.017	0.019	0.011	0.015	0.014	0.013	0.042	0.042	0.012	0.006	0.011	0.009	0.012	0.012	0.013	0.012	0.016	0.010	0.013
Fe^{3+}	0.165	0.087	0.066	0.249	0.052	0.106	0.136	0.121	0.016	0.000	0.000	0.146	0.146	0.154	0.000	0.000	0.056	0.065	0.055	0.061	0.068	0.067
Mg	4.360	4.359	4.330	4.284	4.364	4.299	4.250	4.206	4.937	5.658	5.193	4.587	4.523	4.441	4.917	4.960	4.906	4.881	4.912	4.946	4.873	4.912
Fe^{2+}	0.029	0.113	0.153	0.002	0.179	0.108	0.090	0.086	0.000	0.029	0.025	0.000	0.000	0.000	0.057	0.057	0.000	0.000	0.000	0.000	0.000	0.000
Mn	0.004	0.007	0.008	0.002	0.005	0.001	0.004	0.001	0.000	0.002	0.000	0.002	0.000	0.000	0.000	0.000	0.001	0.005	0.000	0.001	0.000	0.001
B:																						
Ca	1.923	1.874	1.878	1.858	1.792	1.901	1.919	1.948	1.828	1.253	1.666	1.886	1.911	1.924	1.982	1.960	1.964	1.910	1.975	1.910	1.934	1.927
Na	0.017	0.019	0.008	0.072	0.000	0.000	0.000	0.000	0.190	0.000	0.067	0.068	0.056	0.071	0.018	0.007	0.036	0.086	0.025	0.039	0.066	0.045
A:																						
Ca	0.000	0.000	0.000	0.000	0.052	0.050	0.036	0.020	0.000	0.277	0.000	0.000	0.000	0.000	0.000	0.000	0.000	0.000	0.000	0.000	0.000	0.000
Na	0.326	0.402	0.443	0.419	0.490	0.438	0.442	0.475	0.102	0.370	0.255	0.252	0.310	0.356	0.027	0.041	0.029	0.000	0.062	0.039	0.023	0.045
K	0.010	0.000	0.005	0.018	0.004	0.006	0.009	0.005	0.002	0.005	0.005	0.029	0.025	0.040	0.002	0.003	0.001	0.007	0.002	0.000	0.007	0.004
Mg#	95.8	95.6	95.2	94.5	95.0	95.3	95.0	95.3	99.7	99.5	99.5	96.9	96.9	96.7	98.9	98.9	98.9	98.7	98.9	98.8	98.6	98.6
T (°C)	875	884	893	906	918	915	917	925	748	761	756	840	855	883	724	725	735	741	742	743	747	748
H_2O	4.60	3.28	2.88	5.44	2.90	3.80	4.24	4.10	4.54	6.61	4.65	4.42	3.79	5.15	3.93	4.72	4.22	4.87	5.33	3.51	6.10	4.36

Always consult and cite the final, published document. See http:/www.minsocam.org or GeoscienceWorld

This is the peer-reviewed, final accepted version for American Mineralogist, published by the Mineralogical Society of America.
The published version is subject to change. Cite as Authors (Year) Title. American Mineralogist, in press.
DOI: https://doi.org/10.2138/am-2021-7593. http://www.minsocam.org/

(Table 3 continued)

Sample		18LN07-9-1											18LN07-9-2									
Rock		Chromitite											Chromitite									
Mineral	Amp[1]	Amp[1]	Amp[1]	Amp[1]	Amp[1]	Amp[1]	Amp[1]	Amp[1]	Amp[1]	Amp[1]	Amp[1]	Amp[1]	Amp[1]	Amp[1]	Amp[1]	Amp[1]	Amp[1]	Amp[1]	Amp[1]	Amp[1]	Amp[1]	Amp[1]
Type	Tr	Tr	Tr	Tr	Tr	Tr	Tr	Tr	Tr	Tr	Tr	Tr	Mhb	Tr	Tr	Tr	Tr	Tr	Tr	Tr	Tr	Tr
SiO_2	55.7	58.6	57.4	57.4	57.9	58.2	57.7	56.9	56.0	55.9	56.4	55.9	54.2	58.6	58.2	57.9	57.7	57.3	57.3	57.2	55.5	55.5
TiO_2	0.06	0.02	0.03	0.03	0.05	b.d.l.	0.09	0.07	0.04	0.09	0.04	0.06	0.11	b.d.l.	b.d.l.	0.01	0.03	0.05	0.02	0.03	0.10	0.15
Al_2O_3	1.55	0.41	1.20	0.72	0.89	1.00	0.88	1.58	1.90	1.86	2.46	2.69	3.30	0.15	0.76	1.21	1.08	1.22	1.19	1.62	2.38	2.61
Cr_2O_3	0.67	0.28	0.29	0.14	0.26	0.18	0.29	0.62	0.70	0.67	1.13	0.86	1.08	0.12	0.39	0.30	0.28	0.34	0.72	0.49	0.69	0.95
FeO	0.60	0.51	0.50	0.44	0.50	0.65	1.09	1.19	0.66	1.29	0.55	1.24	1.35	0.57	0.63	0.67	0.57	0.62	0.91	0.62	1.07	1.24
MnO	0.02	0.03	0.01	0.02	0.04	0.04	0.02	0.02	0.01	0.06	0.02	0.02	0.02	b.d.l.	b.d.l.	0.01	0.05	0.04	0.03	0.03	0.02	0.02
MgO	23.5	24.4	23.5	24.2	24.2	24.5	24.5	25.4	23.2	23.5	23.5	23.5	22.7	24.5	24.1	23.9	24.0	23.9	24.4	23.9	22.9	22.8
CaO	12.8	12.9	13.0	12.9	12.8	12.8	12.7	10.3	12.7	12.8	12.7	12.7	12.9	13.1	13.2	12.9	12.9	13.0	12.2	12.9	13.0	12.7
Na_2O	0.45	0.29	0.31	0.45	0.35	0.23	0.37	1.42	0.49	0.64	0.77	0.74	0.98	0.14	0.23	0.33	0.36	0.31	0.39	0.45	0.97	0.67
K_2O	0.02	0.02	b.d.l.	b.d.l.	0.02	0.03	0.02	0.02	0.05	0.10	0.05	0.09	0.12	b.d.l.	b.d.l.	0.04	0.02	0.03	0.04	0.02	0.09	0.06
NiO	0.13	0.10	0.12	0.11	0.16	0.12	0.22	0.21	0.15	0.13	0.11	0.20	0.20	0.10	0.16	0.13	0.17	0.12	0.15	0.17	0.18	0.14
Total	95.6	97.5	96.3	96.4	97.2	97.7	97.8	97.8	95.9	97.1	97.8	98.0	97.0	97.2	97.7	97.4	97.1	97.0	97.4	97.4	96.8	96.9
T(IV):																						
Si	7.740	7.950	7.888	7.881	7.873	7.871	7.850	7.740	7.737	7.690	7.675	7.616	7.498	7.977	7.895	7.866	7.853	7.824	7.807	7.779	7.670	7.642
Al	0.254	0.050	0.112	0.116	0.127	0.129	0.141	0.253	0.264	0.301	0.326	0.384	0.502	0.023	0.105	0.135	0.147	0.176	0.191	0.221	0.330	0.358
Ti	0.006	0.000	0.000	0.003	0.000	0.000	0.009	0.007	0.000	0.009	0.000	0.000	0.000	0.000	0.000	0.000	0.000	0.000	0.002	0.000	0.000	0.000
C(VI):																						
Al	0.000	0.015	0.082	0.000	0.015	0.031	0.000	0.000	0.047	0.000	0.070	0.048	0.036	0.001	0.016	0.059	0.027	0.020	0.000	0.039	0.058	0.065
Ti	0.000	0.002	0.003	0.000	0.005	0.000	0.000	0.000	0.004	0.000	0.004	0.006	0.011	0.000	0.000	0.001	0.003	0.005	0.000	0.003	0.011	0.015
Cr	0.074	0.030	0.032	0.015	0.028	0.019	0.031	0.067	0.076	0.073	0.122	0.093	0.118	0.012	0.042	0.033	0.030	0.037	0.078	0.052	0.075	0.103
Ni+Zn	0.014	0.011	0.014	0.012	0.017	0.014	0.024	0.023	0.017	0.015	0.012	0.022	0.022	0.011	0.017	0.014	0.018	0.013	0.017	0.018	0.020	0.016
Fe^{3+}	0.070	0.058	0.057	0.050	0.057	0.073	0.025	0.057	0.076	0.148	0.062	0.130	0.157	0.047	0.071	0.076	0.065	0.071	0.104	0.071	0.063	0.143
Mg	4.875	4.934	4.822	4.953	4.908	4.940	4.963	5.147	4.786	4.812	4.775	4.783	4.674	4.968	4.880	4.839	4.870	4.871	4.958	4.851	4.710	4.685
Fe^{2+}	0.000	0.000	0.000	0.000	0.000	0.000	0.099	0.078	0.000	0.000	0.000	0.011	0.000	0.018	0.000	0.000	0.000	0.000	0.000	0.000	0.060	0.000
Mn	0.002	0.003	0.001	0.002	0.004	0.004	0.002	0.003	0.001	0.007	0.003	0.002	0.002	0.000	0.000	0.002	0.006	0.005	0.003	0.003	0.003	0.003
B:																						
Ca	1.909	1.869	1.907	1.892	1.870	1.854	1.850	1.501	1.884	1.888	1.857	1.851	1.914	1.907	1.913	1.883	1.886	1.901	1.788	1.887	1.918	1.881
Na	0.055	0.076	0.083	0.076	0.093	0.060	0.008	0.125	0.110	0.057	0.096	0.055	0.066	0.037	0.061	0.086	0.095	0.078	0.052	0.077	0.082	0.090
A:																						
Ca	0.000	0.000	0.000	0.000	0.000	0.000	0.000	0.000	0.000	0.000	0.000	0.000	0.000	0.000	0.000	0.000	0.000	0.000	0.000	0.000	0.000	0.000
Na	0.067	0.000	0.000	0.045	0.000	0.000	0.091	0.250	0.021	0.115	0.106	0.141	0.198	0.000	0.000	0.000	0.000	0.003	0.051	0.041	0.178	0.089
K	0.004	0.003	0.000	0.000	0.003	0.005	0.003	0.004	0.008	0.018	0.008	0.015	0.022	0.000	0.000	0.007	0.004	0.005	0.007	0.004	0.016	0.010
Mg#	98.6	98.8	98.8	99.0	98.9	98.5	97.6	97.4	98.4	97.0	98.7	97.1	96.8	98.7	98.6	98.5	98.7	98.6	97.9	98.6	97.4	97.0
T (°C)	762	730	739	744	742	737	742	783	763	768	779	781	803	721	734	741	744	746	748	756	782	777
H_2O	4.44	2.48	3.65	3.63	2.80	2.33	2.19	2.22	4.10	2.92	2.23	2.01	3.02	2.77	2.29	2.64	2.87	3.02	2.63	2.57	3.20	3.11

Always consult and cite the final, published document. See http:/www.minsocam.org or GeoscienceWorld

This is the peer-reviewed, final accepted version for American Mineralogist, published by the Mineralogical Society of America.
The published version is subject to change. Cite as Authors (Year) Title. American Mineralogist, in press.
DOI: https://doi.org/10.2138/am-2021-7593. http://www.minsocam.org/

(Table 3 continued)

Sample	18LN07-10					
Rock	Chromitite					
Mineral	Amp[1]	Amp[1]	Amp[1]	Amp[1]	Amp[1]	
Type	Tr	Tr	Tr	Tr	Tr	DL
SiO_2	55.4	57.8	57.8	57.4	56.4	0.01
TiO_2	0.11	b.d.l.	0.01	0.08	b.d.l.	0.02
Al_2O_3	2.54	0.16	0.35	0.80	1.17	0.01
Cr_2O_3	1.05	0.07	0.23	0.12	0.37	0.03
FeO	1.46	0.52	0.40	0.40	0.47	0.01
MnO	b.d.l.	b.d.l.	b.d.l.	0.01	0.02	0.06
MgO	22.8	24.1	24.4	24.0	23.4	0.06
CaO	12.8	13.2	13.3	13.4	13.3	0.02
Na_2O	0.65	0.14	0.19	0.42	0.36	0.03
K_2O	0.05	0.01	b.d.l.	0.01	0.02	0.02
NiO	0.12	0.07	0.12	0.10	0.10	0.03
Total	97.0	96.1	96.8	96.6	95.6	
T(IV):						
Si	7.627	7.975	7.943	7.885	7.841	
Al	0.373	0.026	0.056	0.116	0.159	
Ti	0.000	0.000	0.001	0.000	0.000	
C(VI):						
Al	0.039	0.000	0.000	0.015	0.033	
Ti	0.012	0.000	0.000	0.008	0.000	
Cr	0.115	0.008	0.024	0.013	0.040	
Ni+Zn	0.013	0.008	0.014	0.011	0.011	
Fe^{3+}	0.155	0.003	0.000	0.018	0.013	
Mg	4.688	4.958	4.992	4.907	4.858	
Fe^{2+}	0.012	0.058	0.046	0.028	0.041	
Mn	0.000	0.000	0.000	0.001	0.002	
B:						
Ca	1.896	1.955	1.924	1.970	1.985	
Na	0.071	0.012	0.000	0.030	0.015	
A:						
Ca	0.000	0.000	0.035	0.000	0.000	
Na	0.104	0.025	0.050	0.082	0.083	
K	0.008	0.002	0.001	0.002	0.003	
Mg#	96.5	98.8	99.1	99.1	98.9	
T (°C)	776	722	729	744	746	
H_2O	3.00	3.92	3.23	3.37	4.40	

Always consult and cite the final, published document. See http:/www.minsocam.org or GeoscienceWorld

This is the peer-reviewed, final accepted version for American Mineralogist, published by the Mineralogical Society of America.
The published version is subject to change. Cite as Authors (Year) Title. American Mineralogist, in press.
DOI: https://doi.org/10.2138/am-2021-7593. http://www.minsocam.org/

Note:

Amp[1]: interstitial amphibole; Amp[2]: large amphibole grain in dunite; Amp[3]: amphibole inclusion in the chromite; Tr: tremolite; Mhb: magnesiohornblende; Ed: edenite.

The formula of amphibole is calculated after Ridolfi et al. (2018).

T: Crystallization temperatures of amphibole are estimated after thermometer defined by Putirka (2016).

Always consult and cite the final, published document. See http:/www.minsocam.org or GeoscienceWorld